CMS-EXO-12-034

Search for disappearing tracks in proton-proton collisions at $\sqrt{s} = 8\,\text{TeV}$

The CMS Collaboration[*]

Abstract

A search is presented for long-lived charged particles that decay within the CMS detector and produce the signature of a disappearing track. Disappearing tracks are identified as those with little or no associated calorimeter energy deposits and with missing hits in the outer layers of the tracker. The search uses proton-proton collision data recorded at $\sqrt{s} = 8\,\text{TeV}$ that corresponds to an integrated luminosity of $19.5\,\text{fb}^{-1}$. The results of the search are interpreted in the context of the anomaly-mediated supersymmetry breaking (AMSB) model. The number of observed events is in agreement with the background expectation, and limits are set on the cross section of direct electroweak chargino production in terms of the chargino mass and mean proper lifetime. At 95% confidence level, AMSB models with a chargino mass less than $260\,\text{GeV}$, corresponding to a mean proper lifetime of $0.2\,\text{ns}$, are excluded.

[*]See Appendix B for the list of collaboration members

arXiv:1411.6006v2 [hep-ex] 22 Jan 2015

1 Introduction

We present a search for long-lived charged particles that decay within the tracker volume and produce the signature of a *disappearing track*. A disappearing track can be produced in beyond the standard model (BSM) scenarios by a charged particle whose decay products are undetected. This occurs because the decay products are either too low in momentum to be reconstructed or neutral (and weakly interacting) such that they do not interact with the tracker material or deposit significant energy in the calorimeters.

There are many BSM scenarios that produce particles that manifest themselves as disappearing tracks [1–5]. One example is anomaly-mediated supersymmetry breaking (AMSB) [6, 7], which predicts a particle mass spectrum that has a small mass splitting between the lightest chargino ($\widetilde{\chi}_1^{\pm}$) and the lightest neutralino ($\widetilde{\chi}_1^0$). The chargino can then decay to a neutralino and a pion, $\widetilde{\chi}_1^{\pm} \to \widetilde{\chi}_1^0 \pi^{\pm}$. The phase space for this decay is limited by the small chargino-neutralino mass splitting. As a consequence, the chargino has a significant lifetime, and the daughter pion has momentum of $\approx$100 MeV, typically too low for its track to be reconstructed. For charginos that decay inside the tracker volume, this results in a disappearing track. We benchmark our search in terms of its sensitivity to the chargino mass and chargino-neutralino mass splitting (or equivalently, the chargino mean proper lifetime, τ) in AMSB. Constraints are also placed on the chargino mass and mean proper lifetime for direct electroweak chargino-chargino and chargino-neutralino production.

Previous CMS analyses have searched for long-lived charged particles based on the signature of anomalous ionization energy loss [8–10], but none has targeted a disappearing track signature. A search for disappearing tracks conducted by the ATLAS Collaboration excludes at 95% confidence level (CL) a chargino in AMSB scenarios with mass less than 270 GeV and mean proper lifetime of approximately 0.2 ns [11].

2 Detector description and event reconstruction

The central feature of the CMS apparatus is a superconducting solenoid of 6 m internal diameter. Within the superconducting solenoid volume are a silicon pixel and strip tracker, a lead tungstate crystal electromagnetic calorimeter (ECAL), and a brass and scintillator hadron calorimeter (HCAL), each composed of a barrel and two endcap sections. Extensive forward calorimetry complements the coverage provided by the barrel and endcap detectors. The ECAL consists of 75 848 crystals that provide coverage in pseudorapidity $|\eta| < 1.479$ in the barrel region and $1.479 < |\eta| < 3.0$ in the two endcap regions. Muons are measured in gas-ionization detectors embedded in the steel flux-return yoke outside the solenoid. They are measured in the pseudorapidity range $|\eta| < 2.4$, with detection planes made using three technologies: drift tubes, cathode strip chambers, and resistive plate chambers. Muons are identified as a track in the central tracker consistent with either a track or several hits in the muon system.

The silicon tracker measures ionization energy deposits ("hits") from charged particles within the pseudorapidity range $|\eta| < 2.5$. It consists of 1440 silicon pixel and 15 148 silicon strip detector modules and is located in the 3.8 T field of the superconducting solenoid. The pixel detector has three barrel layers and two endcap disks, and the strip tracker has ten barrel layers and three small plus nine large endcap disks. Isolated particles with transverse momentum p_T = 100 GeV emitted in the range $|\eta| < 1.4$ have track resolutions of 2.8% in p_T and 10 (30) μm in the transverse (longitudinal) impact parameter [12].

The particle-flow (PF) event reconstruction consists in reconstructing and identifying each sin-

gle particle with an optimized combination of all subdetector information [13, 14]. The energy of photons is obtained directly from the ECAL measurement, corrected for zero-suppression effects. The energy of electrons is determined from a combination of the track momentum at the main interaction vertex, the corresponding ECAL cluster energy, and the energy sum of all bremsstrahlung photons attached to the track. The energy of muons is taken from the corresponding track momentum. The energy of charged hadrons is determined from a combination of the track momentum and the corresponding ECAL and HCAL energies, corrected for zero-suppression effects and for the response function of the calorimeters to hadronic showers. Finally, the energy of neutral hadrons is obtained from the corresponding corrected ECAL and HCAL energies.

Particles are clustered into jets using the anti-k_T algorithm [15] with a distance parameter of 0.5. Jet momentum is determined from the vectorial sum of all particle momenta in the jet, and is found from simulation to be within 5% to 10% of the true momentum over the whole p_T spectrum and detector acceptance. An offset correction is applied to take into account the extra energy clustered in jets due to additional proton-proton (pp) interactions within the same bunch crossing. Jet energy corrections are derived from the simulation, and are confirmed using in situ measurements of the energy balance of dijet and photon+jet events.

The missing transverse energy $\not{E}_T$ is defined as the magnitude of the vector sum of the p_T of all PF candidates reconstructed in the event. A more detailed description of the CMS apparatus and event reconstruction, together with a definition of the coordinate system used and the relevant kinematic variables, can be found in Ref. [16].

3 Data samples and simulation

The search is performed with $\sqrt{s} = 8$ TeV pp collision data recorded in 2012 with the CMS detector at the CERN LHC. The data correspond to an integrated luminosity of 19.5 fb^{-1}. A BSM particle that produces a disappearing track would not be identified as a jet or a particle by the PF algorithm because the track is not matched to any activity in the calorimeter or muon systems. To record such particles with the available triggers, we require one or more initial-state-radiation (ISR) jets, against which the BSM particles recoil. As a result, the $\not{E}_T$ is approximately equal to the p_T of the BSM particles, and likewise to the p_T of the ISR jets. To maximize efficiency for the BSM signal, events used for the search are collected with the union of two triggers that had the lowest $\not{E}_T$ thresholds available during the data taking period. The first requires $\not{E}_T > 120$ GeV, where the $\not{E}_T$ is calculated using the calorimeter information only. The second trigger requires $\not{E}_T$ larger than either 95 or 105 GeV, depending on the run period, where $\not{E}_T$ is reconstructed with the PF algorithm and excludes muons from the calculation. Additionally, the second trigger requires at least one jet with $p_T > 80$ GeV within $|\eta| < 2.6$. The use of alternative $\not{E}_T$ calculations in these triggers is incidental; the $\not{E}_T$ thresholds set for these formulations simply happen to be such that these triggers yield the highest BSM signal efficiency.

Events collected with these triggers are required to pass a set of basic selection criteria. These requirements reduce backgrounds from QCD multijet events and instrumental sources of $\not{E}_T$, which are not well-modeled by the simulation. We require $\not{E}_T > 100$ GeV, near the trigger threshold, to maximize the signal acceptance, and at least one jet reconstructed with the PF algorithm with $p_T > 110$ GeV. The jet must have $|\eta| < 2.4$ and meet several criteria aimed at reducing instrumental noise: less than 70% of its energy assigned to neutral hadrons or photons, less than 50% of its energy associated with electrons, and more than 20% of its energy

carried by charged hadrons. Additional jets in the event with $p_T > 30\,\text{GeV}$ and $|\eta| < 4.5$ are allowed provided they meet two additional criteria. To reduce the contribution of QCD multijets events, the difference in azimuthal angle, $\Delta\phi$, between any two jets in the event must be less than 2.5 radians, and the minimum $\Delta\phi$ between the $\not{E}_T$ vector and either of the two highest-p_T jets is required to be greater than 0.5 radians.

Signal samples are simulated with PYTHIA 6 [17] for the processes $q\overline{q}' \rightarrow \widetilde{\chi}_1^\pm \widetilde{\chi}_1^0$ and $q\overline{q} \rightarrow \widetilde{\chi}_1^\pm \widetilde{\chi}_1^\mp$ in the AMSB framework. The SUSY mass spectrum in AMSB is determined by four parameters: the gravitino mass $m_{3/2}$, the universal scalar mass m_0, the ratio of the vacuum expectation values of the Higgs field at the electroweak scale $\tan\beta$, and the sign of the higgsino mass term $\text{sgn}(\mu)$. Of these, only $m_{3/2}$ significantly affects the chargino mass. We produce samples with variations of the $m_{3/2}$ parameter that correspond to chargino masses between 100 and 600 GeV. Supersymmetric particle mass spectra are calculated according to the SUSY Les Houches accord [18] with ISAJET 7.80 [19]. The branching fraction of the $\widetilde{\chi}_1^\pm \rightarrow \widetilde{\chi}_1^0 \pi^\pm$ decay is set to 100%. While the chargino mean proper lifetime is uniquely determined by the four parameters above, the simulation is performed with a variety of mean proper lifetime values ranging from 0.3 to 300 ns to expand the search beyond the AMSB scenario.

To study the backgrounds, we use simulated samples of the following standard model (SM) processes: W+jets, $t\overline{t}$, $Z \rightarrow \ell\ell$ ($\ell = e, \mu, \tau$), $Z \rightarrow \nu\nu$; WW, ZZ, WZ, Wγ, and Zγ boson pair production; and QCD multijet and single-top-quark production. The W+jets and $t\overline{t}$ are generated using MADGRAPH 5 [20] with PYTHIA 6 for parton showering and hadronization, while single top production is modeled using POWHEG [21–24] and PYTHIA 6. The $Z \rightarrow \ell\ell$, boson pair productions, and QCD multijet events are simulated using PYTHIA 6.

All samples are simulated with CTEQ6L1 parton density functions (PDF). The full detector simulation with GEANT4 [25] is used to trace particles through the detector and to model the detector response. Additional pp interactions within a single bunch crossing (pileup) are modelled in the simulation, and the mean number per event is reweighted to match the number observed in data.

4 Background characterization

In the following sections we examine the sources of both physics and instrumental backgrounds to this search. We consider how a disappearing track signature may be produced, that is, a high-momentum ($p_T > 50\,\text{GeV}$), isolated track without hits in the outer layers of the tracker and with little associated energy ($< 10\,\text{GeV}$) deposited in the calorimeters. Various mechanisms that lead to tracks with missing outer hits are described, and the reconstruction limitations that impact each background category are investigated.

4.1 Sources of missing outer hits

A disappearing track is distinguished by missing outer hits in the tracker, N_{outer}, those expected but not recorded after the last (farthest from the interaction point) hit on a track. They are calculated based on the tracker modules traversed by the track trajectory, and they do not include modules known to be inactive. Standard model particles can produce tracks with missing outer hits as the result of interactions with the tracker material. An electron that transfers a large fraction of its energy to a bremsstrahlung photon can change its trajectory sufficiently that subsequent hits are not associated with the original track. A charged hadron that interacts with a nucleus in the detector material can undergo charge exchange, for example via $\pi^+ + n \rightarrow \pi^0 + p$, or can experience a large momentum transfer. In such cases, the track from

the charged hadron may have no associated hits after the nuclear interaction.

There are also several sources of missing outer hits that arise from choices made by the default CMS tracking algorithms, which are employed in this analysis. These allow for the possibility of missing outer hits on the tracks of particles that traverse all of the layers of the tracker, mimicking the signal. In a sample of simulated single-muon events we find that 11% of muons produce tracks that have at least one missing outer hit. This effect occurs not only with muons, but with any type of particle, and thus produces a contribution to each of the SM backgrounds.

The CMS track reconstruction algorithm identifies many possible trajectory candidates, each constructed with different combinations of hits. In the case of multiple overlapping trajectories, a single trajectory is selected based on the number of recorded hits, the number of expected hits not recorded, and the fit χ^2. We find that for most of the selected trajectories with missing outer hits, there exists another candidate trajectory without missing outer hits.

We have identified how a trajectory with missing outer hits is chosen as the reconstructed track over a trajectory with no missing outer hits. The predominant mechanism is that the particle passes through a glue joint of a double sensor module, a region of inactive material that does not record one of the hits in between the first and last hit on the track. Such a trajectory has no missing outer hits, but it does have one expected hit that is not recorded. The penalty for missing hits before the last recorded hit is greater than for those missing after the last hit. As a result, the reconstructed track is instead identified as a trajectory that stops before the layer with the glue joint and has multiple missing outer hits. In a smaller percentage of events, a trajectory with missing outer hits is chosen because its χ^2 is much smaller than that of a trajectory with no missing outer hits.

4.2   Electrons

We reject any tracks matched to an identified electron, but an electron may fail to be identified if its energy is not fully recorded by the ECAL. We study unidentified electrons with a $Z \to e^+e^-$ tag-and-probe [26] data sample in which the tag is a well-identified electron, the probe is an isolated track, and the invariant mass of the tag electron and probe track is consistent with that of a Z boson. From the η, ϕ distribution of probe tracks that fail to be identified as electrons we characterize several ways that an electron's energy can be lost. An electron is more likely to be unidentified if it is directed toward the overlap region between the barrel and endcap of the ECAL or toward the thin gaps between cylindrical sections of the barrel ECAL. We therefore reject tracks pointing into these regions. An electron may also fail the identification if it is directed towards an ECAL channel that is inoperational or noisy, so we remove tracks that are near any such known channels. After these vetoes, concentrations of unidentified electrons in a few regions survive. Thus we also veto tracks in these additional specific regions.

4.3   Muons

To reduce the background from muons, we veto tracks that are matched to a muon meeting loose identification criteria.

We study muons that fail this identification with a $Z \to \mu^+\mu^-$ tag-and-probe data sample. The probe tracks are more likely to fail the muon identification in the region of the gap between the first two "wheels" of the barrel muon detector, $0.15 < |\eta| < 0.35$; the region of gaps between the inner and outer "rings" of the endcap muon disks, $1.55 < |\eta| < 1.85$; and in regions near a problematic muon chamber. Tracks in these regions are therefore excluded.

With a sample of simulated single-muon events we investigate the signatures of muons outside

these fiducial regions that fail to be identified. In this sample the muon reconstruction inefficiency is 6.8×10^{-5}. We identify three signatures of unreconstructed muons. One signature is a large ECAL deposit or a large HCAL deposit. In a second signature, there are reconstructed muon segments in the muon detectors that fail to be matched to the corresponding tracker track. The final signature has no recorded muon detector segments or calorimeter deposits. These signatures are consistent with a $\mu \to e\nu\bar{\nu}$ decay in flight or a secondary electromagnetic shower. Lost muons that produce large calorimeter deposits are rejected, while the contribution from those without calorimeter deposits is estimated from control samples in data.

4.4   Hadrons

Charged hadrons can produce tracks with missing outer hits as a result of a nuclear interaction. However, tracks produced by charged hadrons in quark/gluon jets typically fail the requirements that the track be isolated and have little associated calorimeter energy. According to simulation, the contribution from hadrons in jets in the search sample is ten times smaller than that of the hadrons from a single-prong hadronic tau (τ_h) decay. The track from a τ_h lepton decay can satisfy the criteria of little associated calorimeter energy but large p_T if the p_T of the hadron is mismeasured, i.e. measured to be significantly larger than the true value. This class of background is studied using a sample of simulated single-pion events.

In these events, the pion tracks typically have $\approx$17 hits. From this original sample we produce three new samples in which all hits associated with the track after the 5th, 6th, or 7th innermost hit have been removed. After repeating the reconstruction, the associated calorimeter energy does not change with the removal of hits on the track. However, the p_T resolution improves with the number of hits on the track, as additional hits provide a greater lever arm to measure the track curvature. Thus the background from τ_h decays is largest for tracks with small numbers of hits, which motivates a minimum number of hits requirement.

4.5   Fake tracks

Fake tracks are formed from combinations of hits that are not produced by a single particle. We obtain a sample of such tracks from simulated events that contain a track that is not matched to any generated particle. Most of these tracks have only three or four hits; the probability to find a combination of hits to form a fake track decreases rapidly with the number of hits on the track. However, fake tracks typically are missing many outer hits and have little associated calorimeter energy, so they closely resemble signal tracks.

5   Candidate track selection

In this section, we define the *candidate track* criteria that are designed to suppress the backgrounds described in the previous section and to identify well-reconstructed, prompt tracks with large p_T. The candidate track sample is composed of the events that pass the basic selection defined in Section 3 and contain a track that meets the following criteria.

A candidate track is required to have $p_T > 50\,\text{GeV}$ and $|\eta| < 2.1$, as signal tracks would typically have large p_T and are produced centrally. The primary vertex is chosen as the one with the largest sum p_T^2 of the tracks associated to it. The track is required to have $|d_0| < 0.02\,\text{cm}$ and $|d_z| < 0.5\,\text{cm}$, where d_0 and d_z are the transverse and longitudinal impact parameters with respect to the primary vertex. The track must be reconstructed from at least 7 hits in the tracker. This reduces the backgrounds associated with poorly reconstructed tracks.

The number of missing middle hits, N_{mid}, is the number of hits expected but not found between the first and last hits associated to a track. The number of missing inner hits, N_{inner}, corresponds to lost hits in layers of the tracker closer to the interaction point, i.e. before the first hit on the track. We require $N_{\mathrm{mid}} = 0$ and $N_{\mathrm{inner}} = 0$ to ensure that the track is not missing any hits in the pixel or strip layers before the last hit on the track. Similarly to the calculation of missing outer hits, the determination of missing inner and middle hits accounts for tracker modules known to be inactive. The relative track isolation, $(\Sigma p_{\mathrm{T}}^{\Delta R < 0.3} - p_{\mathrm{T}})/p_{\mathrm{T}}$ must be less than 0.05, where $\Sigma p_{\mathrm{T}}^{\Delta R < 0.3}$ is the scalar sum of the p_{T} of all other tracks within an angular distance $\Delta R = \sqrt{(\Delta \eta)^2 + (\Delta \phi)^2} < 0.3$ of the candidate track. Additionally, we require that there be no jet with $p_{\mathrm{T}} > 30\,\mathrm{GeV}$ within $\Delta R < 0.5$ of the track. The above criteria select high-p_{T} isolated tracks. In events with large $\not{E}_{\mathrm{T}}$, the dominant SM source of high-p_{T} and isolated tracks is from leptons.

We veto any tracks within $\Delta R < 0.15$ of a reconstructed electron with $p_{\mathrm{T}} > 10\,\mathrm{GeV}$; the electron must pass a loose identification requirement. To further reduce the background from electrons, we veto tracks in the regions of larger electron inefficiency described in Section 4.2. These regions are the gap between the barrel and endcap of the ECAL, $1.42 < |\eta| < 1.65$; the intermodule gaps of the ECAL; and all cones with aperture $\Delta R = 0.05$ around inoperational or noisy ECAL channels or clusters of unidentified electrons in the $Z \to e^+ e^-$ sample.

We veto any tracks within $\Delta R < 0.15$ of a muon with $p_{\mathrm{T}} > 10\,\mathrm{GeV}$ that passes a loose identification requirement. We additionally reject tracks in regions of larger muon inefficiency identified in Section 4.3. These regions are $0.15 < |\eta| < 0.35$, $1.55 < |\eta| < 1.85$, and within $\Delta R < 0.25$ of any problematic muon detector.

After vetoing tracks that correspond to reconstructed electrons and muons, we face a background from single-prong τ_{h} decays. We veto any track within $\Delta R < 0.15$ of a reconstructed hadronic tau candidate. The reconstructed tau must have $p_{\mathrm{T}} > 30\,\mathrm{GeV}$, $|\eta| < 2.3$, and satisfy a set of loose isolation criteria.

The background contributions in the candidate track sample, as estimated from Monte Carlo simulations, are summarized in Table 1.

Table 1: The background contributions in the candidate track sample estimated from the simulation by the identity of the generated particle matched to the candidate track.

Source	Contribution
Electrons	15%
Muons	20%
Hadrons	60%
Fake tracks	5%

6   Disappearing track selection

We define a *disappearing track* as a candidate track that has the signature of missing outer hits and little associated calorimeter energy. A disappearing track is first required to have $N_{\mathrm{outer}} \geq 3$. Tracks from the potential signal are generally missing several outer hits, provided their lifetime is such that they decay within the tracker volume. To remove SM sources of tracks with missing outer hits, we additionally require that the associated calorimeter energy E_{calo} of a disappearing track be less than $10\,\mathrm{GeV}$, much smaller than the minimum p_{T} of $50\,\mathrm{GeV}$. Since the decay products of the chargino are too low in momentum to be reconstructed or weakly interacting, they would not deposit significant energy in the calorimeters. We compute E_{calo} as the sum of the ECAL and HCAL clusters within $\Delta R < 0.5$ of the direction of the track.
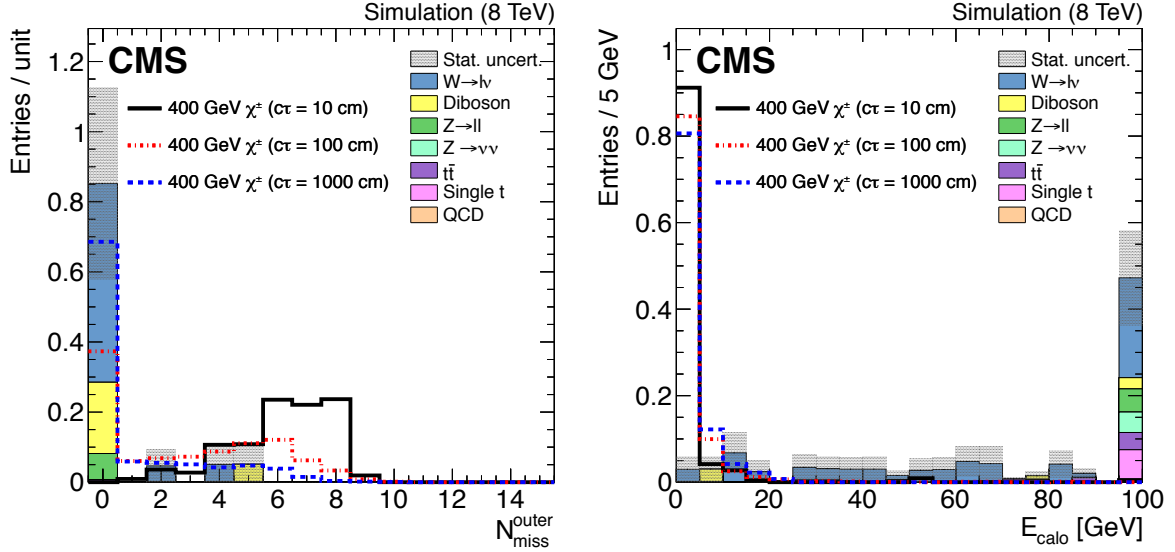
Figure 1: The number of missing outer hits (left) and the associated calorimeter energy (right) of tracks in the search sample, before applying the requirement on the plotted quantity. The signal and the background sum distributions have both been normalized to unit area, and overflow entries are included in the last bin.

The requirements placed on E_{calo} and N_{outer} effectively isolate signal from background, as shown in Fig. 1. Tracks produced by SM particles generally are missing no outer hits and have large E_{calo}, while signal tracks typically have many missing outer hits and very little E_{calo}. The search sample is the subset of events in the candidate track sample that contain at least one disappearing track. The efficiencies to pass various stages of the selection, derived from simulation, are given for signal events in Table 2.

Table 2: Cumulative efficiencies for signal events to pass various stages of the selection.

Chargino mass [GeV]	300	300	300	500	500	500
Chargino $c\tau$ [cm]	10	100	1000	10	100	1000
Trigger	10%	10%	7.4%	13%	13%	10%
Basic selection	7.0%	6.7%	4.2%	8.9%	9.0%	6.3%
High-p_T isolated track	0.24%	3.6%	3.1%	0.14%	4.4%	4.9%
Candidate track	0.15%	2.3%	1.3%	0.10%	2.9%	2.2%
Disappearing track	0.13%	1.0%	0.27%	0.095%	1.4%	0.47%

7 Background estimates and associated systematic uncertainties

For each of the background sources described in Sections 4.2–4.5, the contribution in the search sample is estimated. The SM backgrounds are estimated with a method that is based on data and only relies on simulation to determine the identification inefficiency. The estimate of the fake-track background is obtained from data.

7.1 Standard model backgrounds

We estimate the SM background contributions to the search sample as $N^i = N^i_{ctrl} P^i$, where N^i_{ctrl} is the number of events in data control samples enriched in the given background source and P^i

is the simulated identification inefficiency, for $i = $ e, μ, τ. The electron-enriched control sample is selected by requiring all the search sample criteria except for the electron veto and the E_{calo} requirement. The muon-enriched control sample is selected by requiring all the search sample criteria except for the muon veto. The τ_{h}-enriched control sample is selected by requiring all the search sample criteria except for the τ_{h} veto and the E_{calo} requirement. The E_{calo} requirement is removed for the electron and τ_{h} control samples because it is strongly correlated with both the electron and τ_{h} vetoes. The hadron background is estimated as the contribution from τ_{h} decays, which is its dominant component.

The identification inefficiencies P^i correspond to the probability to survive the corresponding veto criteria, i.e., the electron veto and E_{calo} requirement for electrons, the muon veto for muons, and the τ_{h} veto and E_{calo} requirement for τ leptons. We determine P^i, defined to be the ratio of the number of events of the given background source in the search sample to the number in the corresponding control sample, from the simulated W $\to \ell\nu$+jets process. The W $\to \ell\nu$+jets process is the dominant contribution of the control samples: it represents 84% of the electron-enriched control sample, 85% of the muon-enriched control sample, and 75% of the τ_{h}-enriched control sample. Of the more than 26 million simulated W $\to \ell\nu$+jets events, only one passes the search sample criteria; in that event the disappearing track is produced by a muon in a W $\to \mu\nu$ decay. For the other simulated physics processes, no events are found in the search sample. Since no simulated electron or tau events survive in the search sample, we quote limits at 68% CL on the electron and τ_{h} inefficiencies. The control sample sizes, identification inefficiencies, and background estimates are given in Table 3.

In addition to the uncertainties that result from the finite size of the simulation samples (labeled "statistical"), we also assess systematic uncertainties in the simulation of P^i using tag-and-probe methods. In Z $\to$ e$^+$e$^-$, Z $\to \mu^+\mu^-$, and Z $\to \tau^+\tau^-$ samples, P^i is measured as the probability of a probe track of the given background type to pass the corresponding veto criteria. The difference between data and simulation is taken as the systematic uncertainty.

The probe tracks are required to pass all of the disappearing-track criteria, with a looser requirement of $p_{\text{T}} > 30\,\text{GeV}$, and without the corresponding veto criteria, i.e., the electron veto and E_{calo} requirement for electrons, the muon veto for muons, and the τ_{h} veto and E_{calo} requirement for taus. Additionally, to obtain an adequate sample size, the Z $\to \tau^+\tau^-$ probe tracks are not required to pass the N_{outer} requirement or the isolation requirement of no jet within $\Delta R < 0.5$ of the track. The Z $\to$ e$^+$e$^-$ and Z $\to \mu^+\mu^-$ tag-and-probe samples are collected with single-lepton triggers and require a tag lepton (e or μ) that is well-reconstructed and isolated. The tag lepton and probe track are required to be opposite in charge and to have an invariant mass between 80 and 100 GeV, consistent with a Z $\to \ell\ell$ decay. We measure P^{e} as the fraction of Z $\to$ e$^+$e$^-$ probe tracks that survive the electron veto and E_{calo} requirement and P^{μ} as the fraction of Z $\to \mu^+\mu^-$ probe tracks that survive the muon veto. The Z $\to \tau^+\tau^-$ tag-and-probe sample is designed to identify a tag τ lepton that decays as $\tau \to \mu\nu\overline{\nu}$. This sample is collected with a single-muon trigger and requires a well-reconstructed, isolated tag muon for which the transverse invariant mass of the muon p_{T} and $\not{E}_{\text{T}}$ is less than 40 GeV. The tag muon and probe track are required to be opposite in charge and to have an invariant mass between 40 and 75 GeV, consistent with a Z $\to \tau^+\tau^-$ decay. We measure P^{τ} as the fraction of probe tracks that survive the τ_{h} veto. No probe tracks in the Z $\to \tau^+\tau^-$ data survive both the τ_{h} veto and the E_{calo} requirement, so the E_{calo} requirement is not included in the determination of P^{τ} for the systematic uncertainty.

For each of the tag-and-probe samples, the contamination from sources other than the target Z $\to \ell\ell$ process is estimated from the simulation and is subtracted from both the data and

simulation samples before calculating P^i. The systematic uncertainties in P^i are summarized in Table 3. The systematic uncertainties in the electron and τ_h estimates are incorporated into the 68% CL upper limit on their background contributions according to Ref. [27].

Table 3: The number of events in the data control samples N^i_{ctrl}, the simulated identification inefficiencies P^i, and the resulting estimated contribution in the search sample N^i, for each of the SM backgrounds. The statistical uncertainties originate from the limited size of the simulation samples, while the systematic uncertainties are derived from the differences in P^i between data and simulation in tag-and-probe samples.

	Electrons	Muons	Taus
Criteria removed to select control sample	e veto $E_{calo} < 10\,\text{GeV}$	μ veto	τ_h veto $E_{calo} < 10\,\text{GeV}$
N^i_{ctrl} from data	7785	4138	29
P^i from simulation	$< 6.3 \times 10^{-5}$	$1.6^{+3.6}_{-1.3} \times 10^{-4}$	<0.019
$N^i = N^i_{ctrl} P^i$	$<0.49\,\text{(stat)}$	$0.64^{+1.47}_{-0.53}\,\text{(stat)}$	$<0.55\,\text{(stat)}$
P^i systematic uncertainty	31%	50%	36%
N^i	$<0.50\,\text{(stat+syst)}$	$0.64^{+1.47}_{-0.53}\,\text{(stat)} \pm 0.32\,\text{(syst)}$	$< 0.57\,\text{(stat+syst)}$

7.2 Fake tracks

The fake-track background is estimated as $N^{fake} = N^{basic} P^{fake}$, where $N^{basic} = 1.77 \times 10^6$ is the number of events in data that pass the basic selection criteria, and P^{fake} is the fake-track rate determined in a $Z \to \ell\ell$ ($\ell = $ e or μ) data control sample, a large sample consisting of well-understood SM processes. In the simulation, the probability of an event to contain a fake track that has large transverse momentum and is isolated does not depend on the underlying physics process of the event. The $Z \to \ell\ell$ sample is collected with single-lepton triggers and is selected by requiring two well-reconstructed, isolated leptons of the same flavor that are opposite in charge and have an invariant mass between 80 and 100 GeV, consistent with a $Z \to \ell\ell$ decay. We measure P^{fake} as the probability of an event in the combined $Z \to \ell\ell$ control sample to contain a track that passes the disappearing-track selection. There are two $Z \to \ell\ell$ data events with an additional track that passes the disappearing-track selection, thus P^{fake} is determined to be $(2.0^{+2.7}_{-1.3}) \times 10^{-7}$. The rate of fake tracks with between 3 and 6 hits is consistent between the sample after the basic selection and the $Z \to \ell\ell$ control sample, as shown in Fig. 2. Fake tracks with 5 hits provide a background-enriched sample that is independent of the search sample, in which tracks are required to have 7 or more hits. We use the ratio of the rates of fake tracks with 5 hits between these two samples (including the statistical uncertainty), to assign a systematic uncertainty of 35%. The fake-track background estimate is $N_{fake} = 0.36^{+0.47}_{-0.23}\,\text{(stat)} \pm 0.13\,\text{(syst)}$ events.

7.3 Background estimate validation

The methods used to estimate the backgrounds in the search sample are tested in three control samples: the candidate track sample and E_{calo} and N_{outer} sideband samples. The sideband samples are depleted in signal by applying inverted signal isolation criteria, and the size of the samples is increased by relaxing the track p_T requirement to $p_T > 30\,\text{GeV}$. In the N_{outer} sideband sample, events must pass all criteria of the candidate track sample, and the candidate track must have 2 or fewer missing outer hits. In the E_{calo} sideband sample, events must pass all criteria of the candidate track sample, and the candidate track must have more than 10 GeV of associated calorimeter energy. The backgrounds in each of these control samples are estimated using the methods used to estimate the backgrounds in the search region, with the appropriate
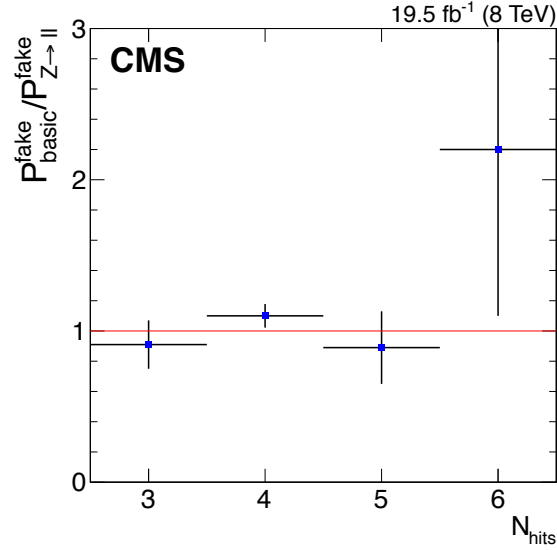
Figure 2: The ratio of the fake-track rates, P^{fake}, in the sample after the basic selection and in the $Z \rightarrow \ell\ell$ control sample, observed in data, as a function of the number of hits on the candidate track.

selection criteria modified to match each sample. The data yields and estimates in each of these samples are consistent within the uncertainties, as shown in Table 4. The methods of background estimation were validated in these control samples before examining the data in the search sample.

Table 4: The data yields and estimated total background in the candidate track sample and the sideband samples.

Sample	Data	Estimate	Data/Estimate
Candidate tracks	59	49.0 ± 5.7	1.20 ± 0.21
E_{calo} sideband	197	195 ± 13	1.01 ± 0.10
N_{outer} sideband	112	103 ± 9	1.09 ± 0.14

8 Additional systematic uncertainties

In addition to the systematic uncertainties in the background estimates described previously, there are systematic uncertainties associated with the integrated luminosity and the signal efficiency.

The integrated luminosity of the 8 TeV pp collision data is measured with a pixel cluster counting method, for which the uncertainty is 2.6% [28].

The uncertainty associated with the simulation of jet radiation is assessed by comparing the recoil of muon pairs from ISR jets in data with a sample of PYTHIA simulated $Z \rightarrow \mu^+\mu^-$ +jets events. The dimuon spectra ratio of data to simulation is used to weight the signal events, and the corresponding selection criteria efficiency is compared to the nominal efficiency. The uncertainty is 3–11%.

We assess uncertainties due to the jet energy scale and resolution from the effect of varying up and down by one standard deviation the jet energy corrections and jet energy resolution smearing parameters [29]. The selection efficiency changes by 0–7% from the variations in the jet energy corrections and jet energy resolution.

We assess the PDF uncertainty by evaluating the envelope of uncertainties of the CTEQ6.6, MSTW08, and NNPDF2.0 PDF sets, according to the PDF4LHC recommendation [30, 31]. The resultant acceptance uncertainties are 1–10%.

The uncertainty associated with the trigger efficiency is assessed with a sample of W $\rightarrow \mu\nu$ events. We compare the trigger efficiency in data and simulation as a function of $\not{E}_T$ reconstructed after excluding muons, as the trigger efficiency is similar for W $\rightarrow \mu\nu$ and signal events. We select W $\rightarrow \mu\nu$ events by applying the basic selection criteria excluding the $\not{E}_T$ requirement. We also apply the candidate track criteria excluding the muon veto. The ratio of the trigger efficiency in data and simulation is used to weight the signal events. The resultant change in the selection efficiency is 1–8%.

The uncertainty associated with the modeling of N_{outer} is assessed by varying the N_{outer} distribution of the simulated signal samples by the disagreement between data and simulation in the N_{outer} distribution in a control sample of muon tracks. Since muons are predominantly affected by the algorithmic sources of missing outer hits described in Section 4.1, they illustrate how well the N_{outer} distribution is modeled in simulation. The consequent change in signal efficiencies is found to be 0–7%.

The uncertainties associated with missing inner and middle hits are assessed as the difference between data and simulation in the efficiency of the requirements of zero missing inner or middle hits in a control sample of muons. A sample of muons is used because they produce tracks that rarely have missing inner or middle hits, as would be the case for signal. These uncertainties are 3% for missing inner hits and 2% for missing middle hits.

The systematic uncertainty associated with the simulation of E_{calo} is assessed as the difference between data and simulation in the efficiency of the $E_{calo} < 10$ GeV requirement, in a control sample of fake tracks with exactly 4 hits. This sample is used because such tracks have very little associated calorimeter energy, as would be the case for signal tracks. The uncertainty is 6%.

The uncertainty associated with the modeling of the number of pileup interactions per bunch crossing is assessed by weighting the signal events to match target pileup distributions in which the numbers of inelastic interactions are shifted up and down by the uncertainty. The consequent variation in the signal efficiency is 0–2%.

The uncertainty in the track reconstruction efficiency is assessed with a tag-and-probe study [32]. The track reconstruction efficiency is measured for probe muons, which are reconstructed using information from the muon system only. We take the uncertainty to be the largest difference between data and simulation among several pseudorapidity ranges, observed to be 2%.

The systematic uncertainties in the signal efficiency for samples of charginos with $c\tau$ in the range of maximum sensitivity, 10–1000 cm, and all simulated masses, are summarized in Table 5.

9 Results

Two data events are observed in the search sample, which is consistent with the expected background. The numbers of expected events from background sources compared with data in the search sample are shown in Table 6. From these results, upper limits at 95% CL on the total production cross section of direct electroweak chargino-chargino and chargino-neutralino produc-

Table 5: Signal efficiency systematic uncertainties, for charginos with masses in the range 100–600 GeV and $c\tau$ of 10–1000 cm.

Jet radiation (ISR)	3–11%
Jet energy scale / resolution	0–7%
PDF	1–10%
Trigger efficiency	1–8%
N_{outer} modeling	0–7%
N_{inner}, N_{mid} modeling	2–3%
E_{calo} modeling	6%
Pileup	0–2%
Track reconstruction efficiency	2%
Total	9–22%

tion are calculated for various chargino masses and mean proper lifetimes. The next-to-leading-order cross sections for these processes, and their uncertainties, are taken from Refs. [33, 34]. The limits are calculated with the CL_S technique [35, 36], using the LHC-type CL_S method [37]. This method uses a test statistic based on a profile likelihood ratio [38] and treats nuisance parameters in a frequentist context. Nuisance parameters for the systematic uncertainties in the integrated luminosity and in the signal efficiency are constrained with log-normal distributions. There are two types of nuisance parameters for the uncertainties in the background estimates, and they are specified separately for each of the four background contributions. Those that result from the limited size of a sample are constrained with gamma distributions, while those that are associated with the relative disagreement between data and simulation in a control region have log-normal constraints. The mean and standard deviation of the distribution of pseudo-data generated under the background-only hypothesis provide an estimate of the total background contribution to the search sample of 1.4 ± 1.2 events.

Table 6: The expected background from all sources compared with data in the search sample.

Event source	Yield	
Electrons	<0.49 (stat)	<0.50 (stat+syst)
Muons	$0.64^{+1.47}_{-0.53}$ (stat) ± 0.32 (syst)	
Taus	<0.55 (stat)	<0.57 (stat+syst)
Fake tracks	$0.36^{+0.47}_{-0.23}$ (stat) ± 0.13 (syst)	
Data	2	

The distributions of the p_T, number of hits, E_{calo}, and N_{outer} of the disappearing tracks in the search region are shown for the observed events and the estimated backgrounds in Fig. 3. The shapes of the electron, muon, and tau background distributions are obtained from the data control samples enriched in the given background. The fake track distribution shapes are taken from the $Z \rightarrow \ell\ell$ control sample, using fake tracks with 5 hits, except for the plot of the number of hits, for which fake tracks with 7 or more hits are used. The background normalizations have the relative contributions of Table 6 and a total equal to 1.4 events, the mean of the background-only pseudo-data. No significant discrepancy between the data and estimated background is found.

In contrast to a slowly moving chargino, which is expected to have a large average ionization energy loss, the energy loss of the two disappearing tracks in the search sample is compatible with that of minimum-ionizing SM particles, ≈ 3 MeV/cm.

The expected and observed constraints on the allowed chargino mean proper lifetime and mass are presented in Fig. 4. The maximum sensitivity is for charginos with a mean proper lifetime
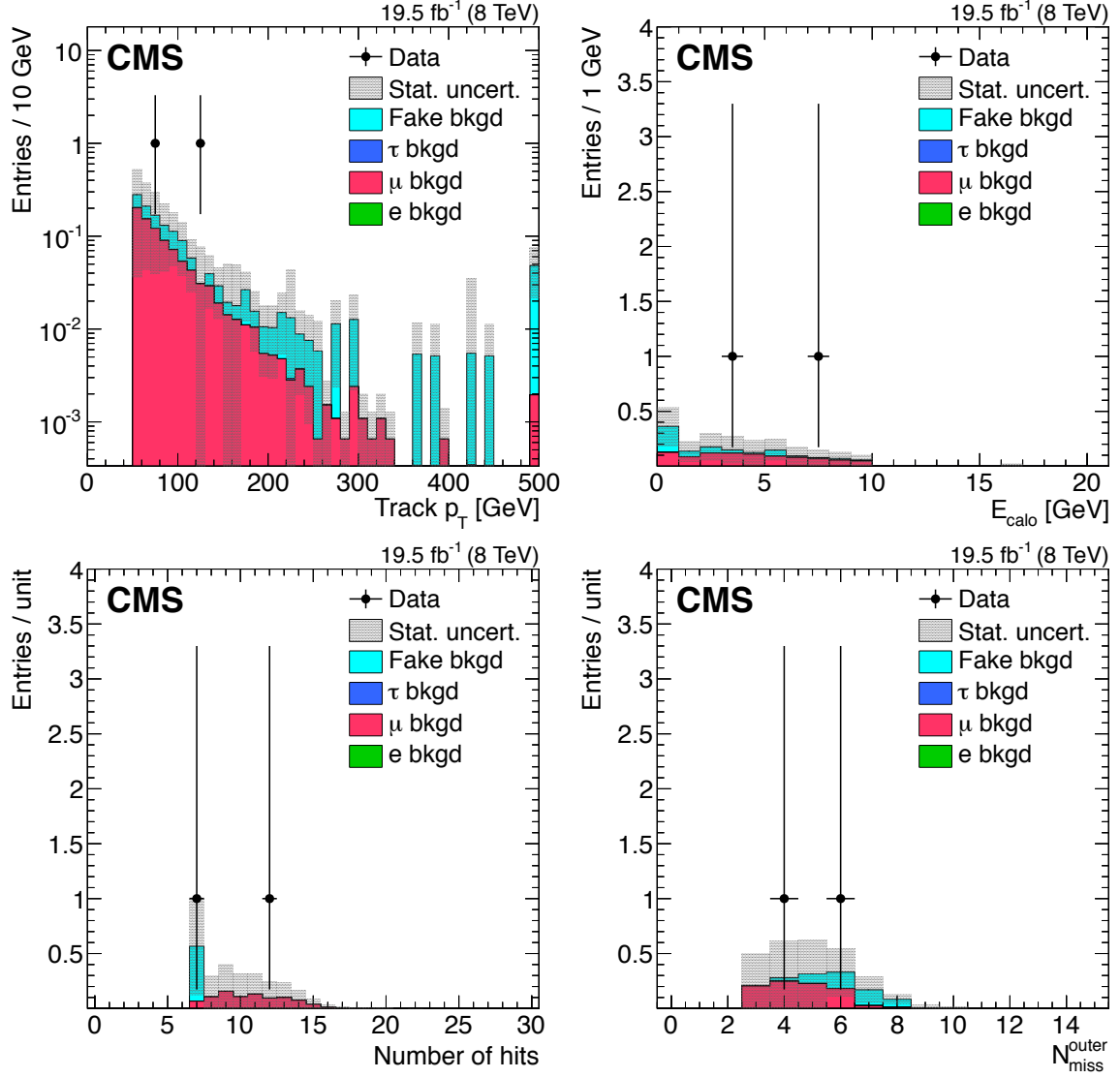
Figure 3: Distributions of the disappearing tracks in the search sample. The estimated backgrounds are normalized to have the relative contributions of Table 6 and a total equal to the mean of the background-only pseudo-data (1.4 events). Histograms for the electron and tau backgrounds are not visible because the central value of their estimated contribution is zero.

of 7 ns, for which masses less than 505 GeV are excluded at 95% CL.

In Fig. 5, we show the expected and observed constraints on the mass of the chargino and the mass difference between the chargino and neutralino, $\Delta m_{\widetilde{\chi}_1} = m_{\widetilde{\chi}_1^\pm} - m_{\widetilde{\chi}_1^0}$, in the minimal AMSB model. The limits on $\tau_{\widetilde{\chi}_1^\pm}$ are converted into limits on $\Delta m_{\widetilde{\chi}_1}$ according to Ref. [39, 40]. The two-loop level calculation of $\Delta m_{\widetilde{\chi}_1}$ for wino-like lightest chargino and neutralino states [41] is also indicated. In the AMSB model, we exclude charginos with mass less than 260 GeV, corresponding to a chargino mean proper lifetime of 0.2 ns and $\Delta m_{\widetilde{\chi}_1} = 160$ MeV.

In Fig. 6, we show the observed upper limit on the total cross section of the $q\overline{q}' \rightarrow \widetilde{\chi}_1^\pm \widetilde{\chi}_1^0$ plus $q\overline{q} \rightarrow \widetilde{\chi}_1^\pm \widetilde{\chi}_1^\mp$ processes in terms of chargino mass and mean proper lifetime. A model-independent interpretation of the results is provided in Appendix A.
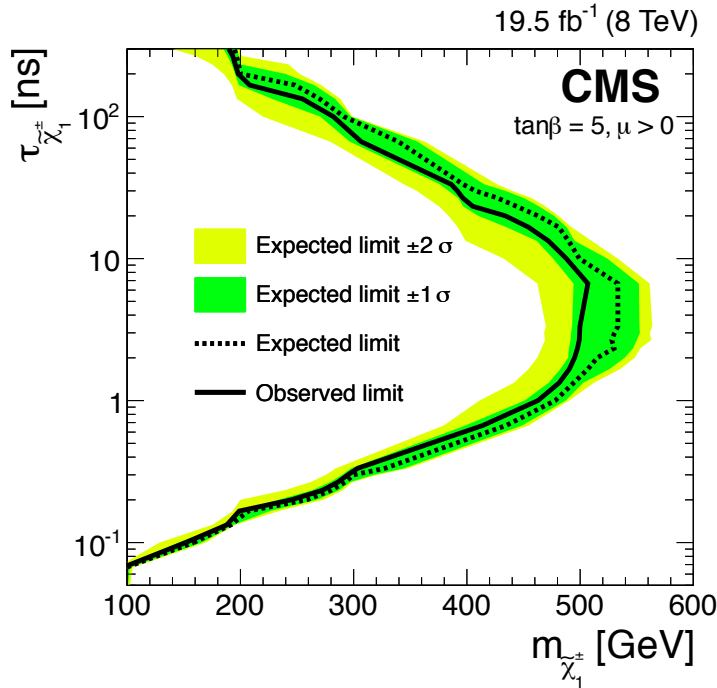
Figure 4: The expected and observed constraints on the chargino mean proper lifetime and mass. The region to the left of the curve is excluded at 95% CL.

10   Summary

A search has been presented for long-lived charged particles that decay within the CMS detector and produce the signature of a disappearing track. In a sample of proton-proton data recorded at a collision energy of $\sqrt{s} = 8$ TeV and corresponding to an integrated luminosity of 19.5 fb^{-1}, two events are observed in the search sample. Thus, no significant excess above the estimated background of 1.4 ± 1.2 events is observed and constraints are placed on the chargino mass, mean proper lifetime, and mass splitting. Direct electroweak production of charginos with a mean proper lifetime of 7 ns and a mass less than 505 GeV is excluded at 95% confidence level. In the AMSB model, charginos with masses less than 260 GeV, corresponding to a mean proper lifetime of 0.2 ns and chargino-neutralino mass splitting of 160 MeV, are excluded at 95% confidence level. These constraints corroborate those set by the ATLAS Collaboration [11].
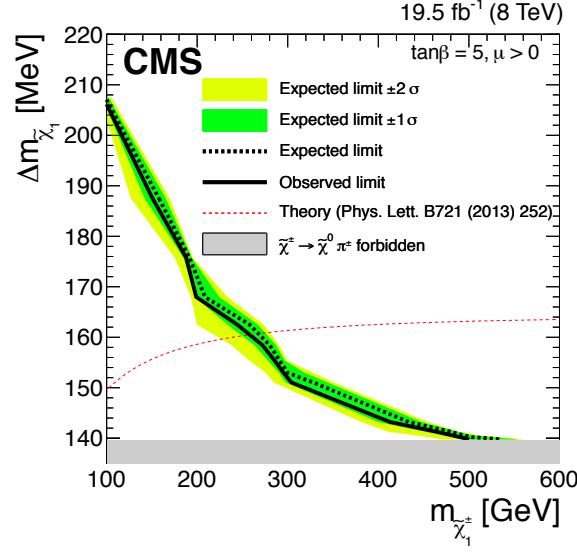
Figure 5: The expected and observed constraints on the chargino mass and the mass splitting between the chargino and neutralino, $\Delta m_{\widetilde{\chi}_1}$, in the AMSB model. The prediction for $\Delta m_{\widetilde{\chi}_1}$ from Ref. [41] is also indicated.
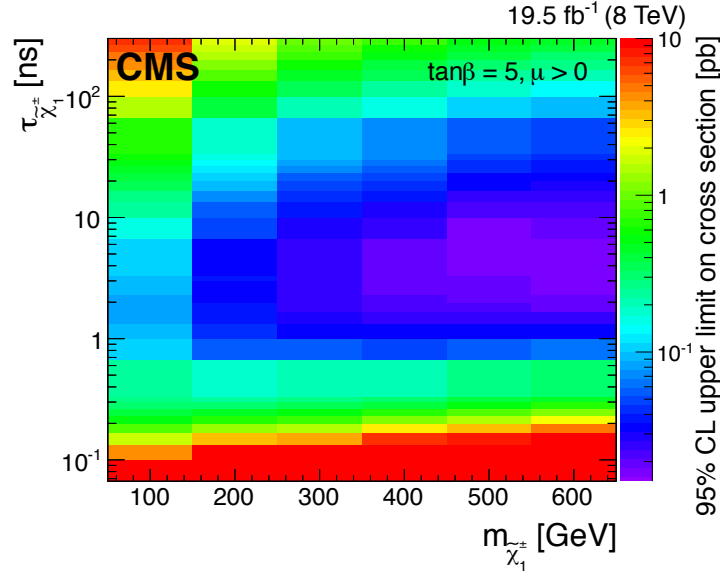

Figure 6: The observed upper limit (in pb) on the total cross section of $q\overline{q}' \rightarrow \widetilde{\chi}_1^{\pm}\widetilde{\chi}_1^0$ and $q\overline{q} \rightarrow \widetilde{\chi}_1^{\pm}\widetilde{\chi}_1^{\mp}$ processes as a function of chargino mass and mean proper lifetime. The simulated chargino mass used to obtain the limits corresponds to the center of each bin.

Acknowledgments

References

[1] M. Ibe, S. Matsumoto, and T. T. Yanagida, "Pure gravity mediation with $m_{3/2} = 10$–100 TeV", *Phys. Rev. D* **85** (2012) 095011, `doi:10.1103/PhysRevD.85.095011`, `arXiv:1202.2253`.

[2] L. J. Hall, Y. Nomura, and S. Shirai, "Spread supersymmetry with $\widetilde{W}$ LSP: gluino and dark matter signals", *JHEP* **01** (2013) 032, `doi:10.1007/JHEP01(2013)036`, `arXiv:1210.2395`.

[3] A. Arvanitaki, N. Craig, S. Dimopoulos, and G. Villadoro, "Mini-Split", *JHEP* **02** (2013) 032, `doi:10.1007/JHEP02(2013)126`, `arXiv:1210.0555`.

[4] N. Arkani-Hamed et al., "Simply unnatural supersymmetry", (2012). `arXiv:1212.6971`.

[5] M. Citron et al., "End of the CMSSM coannihilation strip is nigh", *Phys. Rev. D* **87** (2013) 036012, `doi:10.1103/PhysRevD.87.036012`, `arXiv:1212.2886`.

[6] G. F. Giudice, R. Rattazzi, M. A. Luty, and H. Murayama, "Gaugino mass without singlets", *JHEP* **12** (1998) 027, `doi:10.1088/1126-6708/1998/12/027`, `arXiv:hep-ph/9810442`.

[7] L. Randall and R. Sundrum, "Out of this world supersymmetry breaking", *Nucl. Phys. B* **557** (1999) 79, `doi:10.1016/S0550-3213(99)00359-4`, `arXiv:hep-th/9810155`.

[8] CMS Collaboration, "Search for fractionally charged particles in pp collisions at $\sqrt{s} = 7$ TeV", *Phys. Rev. D* **87** (2012) 092008, `doi:10.1103/PhysRevD.87.092008`.

[9] CMS Collaboration, "Search for heavy long-lived charged particles in pp collisions at $\sqrt{s} = 7$ TeV", *Phys. Lett. B* **713** (2012) 408, `doi:10.1016/j.physletb.2012.06.023`, `arXiv:1205.0272`.

[10] CMS Collaboration, "Searches for long-lived charged particles in pp collisions at $\sqrt{s} = 7$ and 8 TeV", *JHEP* **07** (2013) 122, `doi:10.1007/JHEP07(2013)122`, `arXiv:1305.0491`.

[11] ATLAS Collaboration, "Search for charginos nearly mass degenerate with the lightest neutralino based on a disappearing-track signature in pp collisions at $\sqrt{s} = 8$ TeV with the ATLAS detector", *Phys. Rev. D* **88** (2013) 112006, `doi:10.1103/PhysRevD.88.112006`, `arXiv:1310.3675`.

[12] CMS Collaboration, "Description and performance of track and primary-vertex reconstruction with the CMS tracker", *J. Instrum.* **9** (2014) P10009, `doi:10.1088/1748-0221/9/10/P10009`.

[13] CMS Collaboration, "Commissioning of the Particle-flow Event Reconstruction with the first LHC collisions recorded in the CMS detector", CMS Physics Analysis Summary CMS-PAS-PFT-10-001, 2010.

[14] CMS Collaboration, "Particle–flow event reconstruction in CMS and performance for jets, taus, and E_T^{miss}", CMS Physics Analysis Summary CMS-PAS-PFT-09-001, 2009.

[15] M. Cacciari, G. P. Salam, and G. Soyez, "The anti-k_t jet clustering algorithm", *JHEP* **04** (2008) 063, `doi:10.1088/1126-6708/2008/04/063`, `arXiv:0802.1189`.

[16] CMS Collaboration, "The CMS experiment at the CERN LHC", *JINST* **03** (2008) S08004, `doi:10.1088/1748-0221/3/08/S08004`.

[17] T. Sjöstrand, S. Mrenna, and P. Z. Skands, "PYTHIA 6.4 physics and manual", *JHEP* **05** (2006) 026, `doi:10.1088/1126-6708/2006/05/026`, `arXiv:hep-ph/0603175`.

[18] P. Skands et al., "SUSY Les Houches accord: interfacing SUSY spectrum calculators, decay packages, and event generators", *JHEP* **07** (2004) 036, `doi:10.1088/1126-6708/2004/07/036`, `arXiv:hep-ph/0311123`.

[19] H. Baer, F. E. Paige, S. C. Protopopescu, and X. Tata, "ISAJET 7.48: A Monte Carlo event generator for pp, p$\bar{\text{p}}$, and e$^+$e$^-$ interactions", (2000). `arXiv:hep-ph/0001086`.

[20] J. Alwall et al., "The automated computation of tree-level and next-to-leading order differential cross sections, and their matching to parton shower simulations", *JHEP* **07** (2014) 079, `doi:10.1007/JHEP07(2014)079`, `arXiv:1405.0301`.

[21] S. Alioli, P. Nason, C. Oleari, and E. Re, "NLO single-top production matched with shower in POWHEG: s- and t-channel contributions", *JHEP* **09** (2009) 111, `doi:10.1088/1126-6708/2009/09/111`, `arXiv:0907.4076`. [Erratum: `doi:10.1007/JHEP02(2010)011`].

[22] S. Frixione, P. Nason, and C. Oleari, "Matching NLO QCD computations with Parton Shower simulations: the POWHEG method", *JHEP* **11** (2007) 070, `doi:10.1088/1126-6708/2007/11/070`, `arXiv:0709.2092`.

[23] P. Nason, "A New Method for Combining NLO QCD with Shower Monte Carlo Algorithms", *JHEP* **11** (2004) 040, `doi:10.1088/1126-6708/2004/11/040`, `arXiv:hep-ph/0409146`.

[24] S. Alioli, P. Nason, C. Oleari, and E. Re, "A general framework for implementing NLO calculations in shower Monte Carlo programs: the POWHEG BOX", *JHEP* **06** (2010) 043, `doi:10.1007/JHEP06(2010)043`, `arXiv:1002.2581`.

[25] S. Agostinelli et al., "Geant4—a simulation toolkit", *Nucl. Instrum. Meth. A* **506** (2003) 250, `doi:10.1016/S0168-9002(03)01368-8`.

[26] CMS Collaboration, "Measurements of inclusive W and Z cross sections in pp collisions at $\sqrt{s} = 7$ TeV", *JHEP* **04** (2011) 80, `doi:10.1007/JHEP01(2011)080`, `arXiv:1012.2466`.

[27] R. D. Cousins and V. L. Highland, "Incorporating systematic uncertainties into an upper limit", *Nucl. Instrum. Meth. A* **320** (1992) 331, `doi:10.1016/0168-9002(92)90794-5`.

[28] CMS Collaboration, "CMS Luminosity Based on Pixel Cluster Counting - Summer 2013 Update", CMS Physics Analysis Summary CMS-PAS-LUM-13-001, 2013.

[29] CMS Collaboration, "Determination of jet energy calibration and transverse momentum resolution in CMS", *J. Instrum.* **6** (2011) P11002, `doi:10.1088/1748-0221/6/11/P11002`.

[30] S. Alekhin et al., "The PDF4LHC working group interim report", (2011). `arXiv:1101.0536`.

[31] M. Botje et al., "The PDF4LHC working group interim recommendations", (2011). `arXiv:1101.0538`.

[32] CMS Collaboration, "Measurement of Tracking Efficiency", CMS Physics Analysis Summary CMS-PAS-TRK-10-002, 2010.

[33] W. Beenakker et al., "Production of charginos, neutralinos, and sleptons at hadron colliders", *Phys. Rev. Lett.* **83** (1999) 3780, `doi:10.1103/PhysRevLett.83.3780`, `arXiv:hep-ph/9906298`. [Erratum: `doi:10.1103/PhysRevLett.100.029901`].

[34] M. Krämer et al., "Supersymmetry production cross sections in pp collisions at $\sqrt{s} = 7$ TeV", (2012). `arXiv:1206.2892`.

[35] A. L. Read, "Presentation of search results: the CL_s technique", *J. Phys. G* **28** (2002) 2693, `doi:10.1088/0954-3899/28/10/313`.

[36] T. Junk, "Confidence level computation for combining searches with small statistics", *Nucl. Instrum. Meth. A* **434** (1999) 435, `doi:10.1016/S0168-9002(99)00498-2`, `arXiv:hep-ex/9902006`.

[37] ATLAS and CMS Collaborations, "Procedure for the LHC Higgs boson search combination in Summer 2011", Technical Report ATL-PHYS-PUB 2011-11, CMS NOTE 2011/005, 2011.

[38] G. Cowan, K. Cranmer, E. Gross, and O. Vitells, "Asymptotic formulae for likelihood-based tests of new physics", *Eur. Phys. J. C* **71** (2011) 1554, `doi:10.1140/epjc/s10052-011-1554-0`, `arXiv:1007.1727`.

[39] C. Chen, M. Drees, and J. Gunion, "Searching for invisible and almost invisible particles at e^+e^- colliders", *Phys. Rev. Lett.* **76** (1996) 2002, `doi:10.1103/PhysRevLett.76.2002`, `arXiv:hep-ph/9512230`. [Erratum: `http://arxiv.org/abs/hep-ph/9902309`].

[40] C. Chen, M. Drees, and J. Gunion, "A non-standard string/SUSY scenario and its phenomenological implications", *Phys. Rev. D* **55** (1996) 330, `doi:10.1103/PhysRevD.55.330`, `arXiv:hep-ph/9512230`. [Erratum: `doi:10.1103/PhysRevD.60.039901`].

[41] M. Ibe, S. Matsumoto, and R. Sato, "Mass splitting between charged and neutral winos at two-loop level", *Phys. Lett. B* **721** (2013) 252, `doi:10.1016/j.physletb.2013.03.015`, `arXiv:1212.5989`.

A Model-independent interpretation

To allow the interpretation of the results of this search in the context of other new physics models, the signal efficiency is parameterized in terms of the four-momenta and decay positions of the generated BSM particles. This allows the signal efficiency to be approximated without performing a full simulation of the CMS detector. In this approximation, the signal efficiency is factorized as $\epsilon = \epsilon_b \epsilon_t$, where ϵ_b is the probability of an event to pass the basic selection and ϵ_t is the probability for that event to contain at least one disappearing track. The efficiency to pass the basic selection ϵ_b depends mostly on the p_T of the BSM system, which is approximately equal to $\not{E}_T$. The efficiency of the basic selection as a function of the p_T of the chargino-chargino or chargino-neutralino system p_T ($\widetilde{\chi}\widetilde{\chi}$) is shown in Table 7. To calculate the probability ϵ_t that an event contains a disappearing track, it is necessary to first identify charged particles that pass the following track preselection criteria: $p_T > 50\,\text{GeV}$, $|\eta| < 2.2$, and a decay position within the tracker volume, i.e., with a longitudinal distance to the interaction point of less than $280\,\text{cm}$ and a transverse decay distance in the laboratory frame L_{xy} of less than $110\,\text{cm}$. For long-lived charged particles that meet the track preselection criteria, the efficiency to pass the disappearing-track selection depends mostly on L_{xy}, as given in Table 8. Each of the long-lived BSM particles that pass the preselection should be considered, weighted by its disappearing-track efficiency from Table 8, to determine whether the event contains at least one disappearing track. This parameterization of the efficiency is valid under the assumptions that the long-lived BSM particles are isolated and that their decay products deposit little or no energy in the calorimeters. For the benchmark signal samples used in this analysis, the efficiency approximation agrees with the full simulation efficiencies given in Table 2 within 10% for charginos with $c\tau$ between 10 and 1000 cm. The expected number of signal events N for a new physics process is the product of the signal efficiency ϵ, the cross section σ, and the

integrated luminosity L, $N = \epsilon \sigma L$. By comparing such a prediction with the estimated background of 1.4 ± 1.2 events and the observation of two events in this search, constraints on other models can be set.

Table 7: Efficiency of an event to pass the basic selection. Uncertainties are statistical only.

$p_\mathrm{T}(\tilde{\chi}\tilde{\chi})$ [GeV]	Basic selection efficiency (%)
<100	0.0 ± 0.0
100–125	13.1 ± 0.3
125–150	44.1 ± 0.8
150–175	65.3 ± 1.2
175–200	75.7 ± 1.5
200–225	79.5 ± 1.9
>225	85.5 ± 1.1

Table 8: Efficiency of a track to pass the disappearing-track selection after passing the preselection as a function of the transverse decay distance in the laboratory frame, L_{xy} . Uncertainties are statistical only.

L_{xy} [cm]	Disappearing track efficiency (%)
<30	0.0 ± 0.2
30–40	26.0 ± 1.0
40–50	44.2 ± 1.6
50–70	50.8 ± 1.4
70–80	45.5 ± 2.1
80–90	25.5 ± 1.6
90–110	3.1 ± 0.4
>110	0.0 ± 0.0

B The CMS Collaboration

Yerevan Physics Institute, Yerevan, Armenia
V. Khachatryan, A.M. Sirunyan, A. Tumasyan

Institut für Hochenergiephysik der OeAW, Wien, Austria
W. Adam, T. Bergauer, M. Dragicevic, J. Erö, M. Friedl, R. Frühwirth[1], V.M. Ghete, C. Hartl, N. Hörmann, J. Hrubec, M. Jeitler[1], W. Kiesenhofer, V. Knünz, M. Krammer[1], I. Krätschmer, D. Liko, I. Mikulec, D. Rabady[2], B. Rahbaran, H. Rohringer, R. Schöfbeck, J. Strauss, W. Treberer-Treberspurg, W. Waltenberger, C.-E. Wulz[1]

National Centre for Particle and High Energy Physics, Minsk, Belarus
V. Mossolov, N. Shumeiko, J. Suarez Gonzalez

Universiteit Antwerpen, Antwerpen, Belgium
S. Alderweireldt, S. Bansal, T. Cornelis, E.A. De Wolf, X. Janssen, A. Knutsson, J. Lauwers, S. Luyckx, S. Ochesanu, R. Rougny, M. Van De Klundert, H. Van Haevermaet, P. Van Mechelen, N. Van Remortel, A. Van Spilbeeck

Vrije Universiteit Brussel, Brussel, Belgium
F. Blekman, S. Blyweert, J. D'Hondt, N. Daci, N. Heracleous, J. Keaveney, S. Lowette, M. Maes, A. Olbrechts, Q. Python, D. Strom, S. Tavernier, W. Van Doninck, P. Van Mulders, G.P. Van Onsem, I. Villella

Université Libre de Bruxelles, Bruxelles, Belgium
C. Caillol, B. Clerbaux, G. De Lentdecker, D. Dobur, L. Favart, A.P.R. Gay, A. Grebenyuk, A. Léonard, A. Mohammadi, L. Perniè[2], A. Randle-conde, T. Reis, T. Seva, L. Thomas, C. Vander Velde, P. Vanlaer, J. Wang, F. Zenoni

Ghent University, Ghent, Belgium
V. Adler, K. Beernaert, L. Benucci, A. Cimmino, S. Costantini, S. Crucy, S. Dildick, A. Fagot, G. Garcia, J. Mccartin, A.A. Ocampo Rios, D. Poyraz, D. Ryckbosch, S. Salva Diblen, M. Sigamani, N. Strobbe, F. Thyssen, M. Tytgat, E. Yazgan, N. Zaganidis

Université Catholique de Louvain, Louvain-la-Neuve, Belgium
S. Basegmez, C. Beluffi[3], G. Bruno, R. Castello, A. Caudron, L. Ceard, G.G. Da Silveira, C. Delaere, T. du Pree, D. Favart, L. Forthomme, A. Giammanco[4], J. Hollar, A. Jafari, P. Jez, M. Komm, V. Lemaitre, C. Nuttens, L. Perrini, A. Pin, K. Piotrzkowski, A. Popov[5], L. Quertenmont, M. Selvaggi, M. Vidal Marono, J.M. Vizan Garcia

Université de Mons, Mons, Belgium
N. Beliy, T. Caebergs, E. Daubie, G.H. Hammad

Centro Brasileiro de Pesquisas Fisicas, Rio de Janeiro, Brazil
W.L. Aldá Júnior, G.A. Alves, L. Brito, M. Correa Martins Junior, T. Dos Reis Martins, J. Molina, C. Mora Herrera, M.E. Pol, P. Rebello Teles

Universidade do Estado do Rio de Janeiro, Rio de Janeiro, Brazil
W. Carvalho, J. Chinellato[6], A. Custódio, E.M. Da Costa, D. De Jesus Damiao, C. De Oliveira Martins, S. Fonseca De Souza, H. Malbouisson, D. Matos Figueiredo, L. Mundim, H. Nogima, W.L. Prado Da Silva, J. Santaolalla, A. Santoro, A. Sznajder, E.J. Tonelli Manganote[6], A. Vilela Pereira

Universidade Estadual Paulista [a], Universidade Federal do ABC [b], São Paulo, Brazil
C.A. Bernardes[b], S. Dogra[a], T.R. Fernandez Perez Tomei[a], E.M. Gregores[b], P.G. Mercadante[b], S.F. Novaes[a], Sandra S. Padula[a]

Institute for Nuclear Research and Nuclear Energy, Sofia, Bulgaria
A. Aleksandrov, V. Genchev[2], R. Hadjiiska, P. Iaydjiev, A. Marinov, S. Piperov, M. Rodozov, S. Stoykova, G. Sultanov, M. Vutova

University of Sofia, Sofia, Bulgaria
A. Dimitrov, I. Glushkov, L. Litov, B. Pavlov, P. Petkov

Institute of High Energy Physics, Beijing, China
J.G. Bian, G.M. Chen, H.S. Chen, M. Chen, T. Cheng, R. Du, C.H. Jiang, R. Plestina[7], F. Romeo, J. Tao, Z. Wang

State Key Laboratory of Nuclear Physics and Technology, Peking University, Beijing, China
C. Asawatangtrakuldee, Y. Ban, Q. Li, S. Liu, Y. Mao, S.J. Qian, D. Wang, Z. Xu, W. Zou

Universidad de Los Andes, Bogota, Colombia
C. Avila, A. Cabrera, L.F. Chaparro Sierra, C. Florez, J.P. Gomez, B. Gomez Moreno, J.C. Sanabria

University of Split, Faculty of Electrical Engineering, Mechanical Engineering and Naval Architecture, Split, Croatia
N. Godinovic, D. Lelas, D. Polic, I. Puljak

University of Split, Faculty of Science, Split, Croatia
Z. Antunovic, M. Kovac

Institute Rudjer Boskovic, Zagreb, Croatia
V. Brigljevic, K. Kadija, J. Luetic, D. Mekterovic, L. Sudic

University of Cyprus, Nicosia, Cyprus
A. Attikis, G. Mavromanolakis, J. Mousa, C. Nicolaou, F. Ptochos, P.A. Razis

Charles University, Prague, Czech Republic
M. Bodlak, M. Finger, M. Finger Jr.[8]

Academy of Scientific Research and Technology of the Arab Republic of Egypt, Egyptian Network of High Energy Physics, Cairo, Egypt
Y. Assran[9], S. Elgammal[10], A. Ellithi Kamel[11], A. Radi[12,13]

National Institute of Chemical Physics and Biophysics, Tallinn, Estonia
M. Kadastik, M. Murumaa, M. Raidal, A. Tiko

Department of Physics, University of Helsinki, Helsinki, Finland
P. Eerola, G. Fedi, M. Voutilainen

Helsinki Institute of Physics, Helsinki, Finland
J. Härkönen, V. Karimäki, R. Kinnunen, M.J. Kortelainen, T. Lampén, K. Lassila-Perini, S. Lehti, T. Lindén, P. Luukka, T. Mäenpää, T. Peltola, E. Tuominen, J. Tuominiemi, E. Tuovinen, L. Wendland

Lappeenranta University of Technology, Lappeenranta, Finland
J. Talvitie, T. Tuuva

DSM/IRFU, CEA/Saclay, Gif-sur-Yvette, France
M. Besancon, F. Couderc, M. Dejardin, D. Denegri, B. Fabbro, J.L. Faure, C. Favaro, F. Ferri, S. Ganjour, A. Givernaud, P. Gras, G. Hamel de Monchenault, P. Jarry, E. Locci, J. Malcles, J. Rander, A. Rosowsky, M. Titov

Laboratoire Leprince-Ringuet, Ecole Polytechnique, IN2P3-CNRS, Palaiseau, France
S. Baffioni, F. Beaudette, P. Busson, E. Chapon, C. Charlot, T. Dahms, M. Dalchenko, L. Dobrzynski, N. Filipovic, A. Florent, R. Granier de Cassagnac, L. Mastrolorenzo, P. Miné, I.N. Naranjo, M. Nguyen, C. Ochando, G. Ortona, P. Paganini, S. Regnard, R. Salerno, J.B. Sauvan, Y. Sirois, C. Veelken, Y. Yilmaz, A. Zabi

Institut Pluridisciplinaire Hubert Curien, Université de Strasbourg, Université de Haute Alsace Mulhouse, CNRS/IN2P3, Strasbourg, France
J.-L. Agram[14], J. Andrea, A. Aubin, D. Bloch, J.-M. Brom, E.C. Chabert, C. Collard, E. Conte[14], J.-C. Fontaine[14], D. Gelé, U. Goerlach, C. Goetzmann, A.-C. Le Bihan, K. Skovpen, P. Van Hove

Centre de Calcul de l'Institut National de Physique Nucleaire et de Physique des Particules, CNRS/IN2P3, Villeurbanne, France
S. Gadrat

Université de Lyon, Université Claude Bernard Lyon 1, CNRS-IN2P3, Institut de Physique Nucléaire de Lyon, Villeurbanne, France
S. Beauceron, N. Beaupere, C. Bernet[7], G. Boudoul[2], E. Bouvier, S. Brochet, C.A. Carrillo Montoya, J. Chasserat, R. Chierici, D. Contardo[2], P. Depasse, H. El Mamouni, J. Fan, J. Fay, S. Gascon, M. Gouzevitch, B. Ille, T. Kurca, M. Lethuillier, L. Mirabito, S. Perries, J.D. Ruiz Alvarez, D. Sabes, L. Sgandurra, V. Sordini, M. Vander Donckt, P. Verdier, S. Viret, H. Xiao

E. Andronikashvili Institute of Physics, Academy of Science, Tbilisi, Georgia
L. Rurua

RWTH Aachen University, I. Physikalisches Institut, Aachen, Germany
C. Autermann, S. Beranek, M. Bontenackels, M. Edelhoff, L. Feld, A. Heister, K. Klein, M. Lipinski, A. Ostapchuk, M. Preuten, F. Raupach, J. Sammet, S. Schael, J.F. Schulte, H. Weber, B. Wittmer, V. Zhukov[5]

RWTH Aachen University, III. Physikalisches Institut A, Aachen, Germany
M. Ata, M. Brodski, E. Dietz-Laursonn, D. Duchardt, M. Erdmann, R. Fischer, A. Güth, T. Hebbeker, C. Heidemann, K. Hoepfner, D. Klingebiel, S. Knutzen, P. Kreuzer, M. Merschmeyer, A. Meyer, P. Millet, M. Olschewski, K. Padeken, P. Papacz, H. Reithler, S.A. Schmitz, L. Sonnenschein, D. Teyssier, S. Thüer, M. Weber

RWTH Aachen University, III. Physikalisches Institut B, Aachen, Germany
V. Cherepanov, Y. Erdogan, G. Flügge, H. Geenen, M. Geisler, W. Haj Ahmad, F. Hoehle, B. Kargoll, T. Kress, Y. Kuessel, A. Künsken, J. Lingemann[2], A. Nowack, I.M. Nugent, O. Pooth, A. Stahl

Deutsches Elektronen-Synchrotron, Hamburg, Germany
M. Aldaya Martin, I. Asin, N. Bartosik, J. Behr, U. Behrens, A.J. Bell, A. Bethani, K. Borras, A. Burgmeier, A. Cakir, L. Calligaris, A. Campbell, S. Choudhury, F. Costanza, C. Diez Pardos, G. Dolinska, S. Dooling, T. Dorland, G. Eckerlin, D. Eckstein, T. Eichhorn, G. Flucke, J. Garay Garcia, A. Geiser, P. Gunnellini, J. Hauk, M. Hempel[15], H. Jung, A. Kalogeropoulos, M. Kasemann, P. Katsas, J. Kieseler, C. Kleinwort, I. Korol, D. Krücker, W. Lange, J. Leonard, K. Lipka, A. Lobanov, W. Lohmann[15], B. Lutz, R. Mankel, I. Marfin[15], I.-A. Melzer-Pellmann, A.B. Meyer, G. Mittag, J. Mnich, A. Mussgiller, S. Naumann-Emme, A. Nayak, E. Ntomari,

H. Perrey, D. Pitzl, R. Placakyte, A. Raspereza, P.M. Ribeiro Cipriano, B. Roland, E. Ron, M.Ö. Sahin, J. Salfeld-Nebgen, P. Saxena, T. Schoerner-Sadenius, M. Schröder, C. Seitz, S. Spannagel, A.D.R. Vargas Trevino, R. Walsh, C. Wissing

University of Hamburg, Hamburg, Germany
V. Blobel, M. Centis Vignali, A.R. Draeger, J. Erfle, E. Garutti, K. Goebel, M. Görner, J. Haller, M. Hoffmann, R.S. Höing, A. Junkes, H. Kirschenmann, R. Klanner, R. Kogler, J. Lange, T. Lapsien, T. Lenz, I. Marchesini, J. Ott, T. Peiffer, A. Perieanu, N. Pietsch, J. Poehlsen, T. Poehlsen, D. Rathjens, C. Sander, H. Schettler, P. Schleper, E. Schlieckau, A. Schmidt, M. Seidel, V. Sola, H. Stadie, G. Steinbrück, D. Troendle, E. Usai, L. Vanelderen, A. Vanhoefer

Institut für Experimentelle Kernphysik, Karlsruhe, Germany
C. Barth, C. Baus, J. Berger, C. Böser, E. Butz, T. Chwalek, W. De Boer, A. Descroix, A. Dierlamm, M. Feindt, F. Frensch, M. Giffels, A. Gilbert, F. Hartmann[2], T. Hauth, U. Husemann, I. Katkov[5], A. Kornmayer[2], P. Lobelle Pardo, M.U. Mozer, T. Müller, Th. Müller, A. Nürnberg, G. Quast, K. Rabbertz, S. Röcker, H.J. Simonis, F.M. Stober, R. Ulrich, J. Wagner-Kuhr, S. Wayand, T. Weiler, R. Wolf

Institute of Nuclear and Particle Physics (INPP), NCSR Demokritos, Aghia Paraskevi, Greece
G. Anagnostou, G. Daskalakis, T. Geralis, V.A. Giakoumopoulou, A. Kyriakis, D. Loukas, A. Markou, C. Markou, A. Psallidas, I. Topsis-Giotis

University of Athens, Athens, Greece
A. Agapitos, S. Kesisoglou, A. Panagiotou, N. Saoulidou, E. Stiliaris

University of Ioánnina, Ioánnina, Greece
X. Aslanoglou, I. Evangelou, G. Flouris, C. Foudas, P. Kokkas, N. Manthos, I. Papadopoulos, E. Paradas, J. Strologas

Wigner Research Centre for Physics, Budapest, Hungary
G. Bencze, C. Hajdu, P. Hidas, D. Horvath[16], F. Sikler, V. Veszpremi, G. Vesztergombi[17], A.J. Zsigmond

Institute of Nuclear Research ATOMKI, Debrecen, Hungary
N. Beni, S. Czellar, J. Karancsi[18], J. Molnar, J. Palinkas, Z. Szillasi

University of Debrecen, Debrecen, Hungary
A. Makovec, P. Raics, Z.L. Trocsanyi, B. Ujvari

National Institute of Science Education and Research, Bhubaneswar, India
S.K. Swain

Panjab University, Chandigarh, India
S.B. Beri, V. Bhatnagar, R. Gupta, U.Bhawandeep, A.K. Kalsi, M. Kaur, R. Kumar, M. Mittal, N. Nishu, J.B. Singh

University of Delhi, Delhi, India
Ashok Kumar, Arun Kumar, S. Ahuja, A. Bhardwaj, B.C. Choudhary, A. Kumar, S. Malhotra, M. Naimuddin, K. Ranjan, V. Sharma

Saha Institute of Nuclear Physics, Kolkata, India
S. Banerjee, S. Bhattacharya, K. Chatterjee, S. Dutta, B. Gomber, Sa. Jain, Sh. Jain, R. Khurana, A. Modak, S. Mukherjee, D. Roy, S. Sarkar, M. Sharan

Bhabha Atomic Research Centre, Mumbai, India
A. Abdulsalam, D. Dutta, V. Kumar, A.K. Mohanty[2], L.M. Pant, P. Shukla, A. Topkar

Tata Institute of Fundamental Research, Mumbai, India
T. Aziz, S. Banerjee, S. Bhowmik[19], R.M. Chatterjee, R.K. Dewanjee, S. Dugad, S. Ganguly,
S. Ghosh, M. Guchait, A. Gurtu[20], G. Kole, S. Kumar, M. Maity[19], G. Majumder, K. Mazumdar,
G.B. Mohanty, B. Parida, K. Sudhakar, N. Wickramage[21]

Institute for Research in Fundamental Sciences (IPM), Tehran, Iran
H. Bakhshiansohi, H. Behnamian, S.M. Etesami[22], A. Fahim[23], R. Goldouzian, M. Khakzad,
M. Mohammadi Najafabadi, M. Naseri, S. Paktinat Mehdiabadi, F. Rezaei Hosseinabadi,
B. Safarzadeh[24], M. Zeinali

University College Dublin, Dublin, Ireland
M. Felcini, M. Grunewald

INFN Sezione di Bari [a], Università di Bari [b], Politecnico di Bari [c], Bari, Italy
M. Abbrescia[a,b], C. Calabria[a,b], S.S. Chhibra[a,b], A. Colaleo[a], D. Creanza[a,c], N. De Filippis[a,c],
M. De Palma[a,b], L. Fiore[a], G. Iaselli[a,c], G. Maggi[a,c], M. Maggi[a], S. My[a,c], S. Nuzzo[a,b],
A. Pompili[a,b], G. Pugliese[a,c], R. Radogna[a,b,2], G. Selvaggi[a,b], A. Sharma[a], L. Silvestris[a,2],
R. Venditti[a,b], P. Verwilligen[a]

INFN Sezione di Bologna [a], Università di Bologna [b], Bologna, Italy
G. Abbiendi[a], A.C. Benvenuti[a], D. Bonacorsi[a,b], S. Braibant-Giacomelli[a,b], L. Brigliadori[a,b],
R. Campanini[a,b], P. Capiluppi[a,b], A. Castro[a,b], F.R. Cavallo[a], G. Codispoti[a,b], M. Cuffiani[a,b],
G.M. Dallavalle[a], F. Fabbri[a], A. Fanfani[a,b], D. Fasanella[a,b], P. Giacomelli[a], C. Grandi[a],
L. Guiducci[a,b], S. Marcellini[a], G. Masetti[a], A. Montanari[a], F.L. Navarria[a,b], A. Perrotta[a],
F. Primavera[a,b], A.M. Rossi[a,b], T. Rovelli[a,b], G.P. Siroli[a,b], N. Tosi[a,b], R. Travaglini[a,b]

INFN Sezione di Catania [a], Università di Catania [b], CSFNSM [c], Catania, Italy
S. Albergo[a,b], G. Cappello[a], M. Chiorboli[a,b], S. Costa[a,b], F. Giordano[a,c,2], R. Potenza[a,b],
A. Tricomi[a,b], C. Tuve[a,b]

INFN Sezione di Firenze [a], Università di Firenze [b], Firenze, Italy
G. Barbagli[a], V. Ciulli[a,b], C. Civinini[a], R. D'Alessandro[a,b], E. Focardi[a,b], E. Gallo[a], S. Gonzi[a,b],
V. Gori[a,b], P. Lenzi[a,b], M. Meschini[a], S. Paoletti[a], G. Sguazzoni[a], A. Tropiano[a,b]

INFN Laboratori Nazionali di Frascati, Frascati, Italy
L. Benussi, S. Bianco, F. Fabbri, D. Piccolo

INFN Sezione di Genova [a], Università di Genova [b], Genova, Italy
R. Ferretti[a,b], F. Ferro[a], M. Lo Vetere[a,b], E. Robutti[a], S. Tosi[a,b]

INFN Sezione di Milano-Bicocca [a], Università di Milano-Bicocca [b], Milano, Italy
M.E. Dinardo[a,b], S. Fiorendi[a,b], S. Gennai[a,2], R. Gerosa[a,b,2], A. Ghezzi[a,b], P. Govoni[a,b],
M.T. Lucchini[a,b,2], S. Malvezzi[a], R.A. Manzoni[a,b], A. Martelli[a,b], B. Marzocchi[a,b,2], D. Menasce[a],
L. Moroni[a], M. Paganoni[a,b], D. Pedrini[a], S. Ragazzi[a,b], N. Redaelli[a], T. Tabarelli de Fatis[a,b]

INFN Sezione di Napoli [a], Università di Napoli 'Federico II' [b], Università della Basilicata (Potenza) [c], Università G. Marconi (Roma) [d], Napoli, Italy
S. Buontempo[a], N. Cavallo[a,c], S. Di Guida[a,d,2], F. Fabozzi[a,c], A.O.M. Iorio[a,b], L. Lista[a],
S. Meola[a,d,2], M. Merola[a], P. Paolucci[a,2]

INFN Sezione di Padova [a]**, Università di Padova** [b]**, Università di Trento (Trento)** [c]**, Padova, Italy**
P. Azzi[a], N. Bacchetta[a], D. Bisello[a,b], A. Branca[a,b], R. Carlin[a,b], P. Checchia[a], M. Dall'Osso[a,b], T. Dorigo[a], S. Fantinel[a], M. Galanti[a,b], F. Gasparini[a,b], U. Gasparini[a,b], A. Gozzelino[a], K. Kanishchev[a,c], S. Lacaprara[a], M. Margoni[a,b], A.T. Meneguzzo[a,b], J. Pazzini[a,b], N. Pozzobon[a,b], P. Ronchese[a,b], F. Simonetto[a,b], E. Torassa[a], M. Tosi[a,b], P. Zotto[a,b], A. Zucchetta[a,b], G. Zumerle[a,b]

INFN Sezione di Pavia [a]**, Università di Pavia** [b]**, Pavia, Italy**
M. Gabusi[a,b], S.P. Ratti[a,b], V. Re[a], C. Riccardi[a,b], P. Salvini[a], P. Vitulo[a,b]

INFN Sezione di Perugia [a]**, Università di Perugia** [b]**, Perugia, Italy**
M. Biasini[a,b], G.M. Bilei[a], D. Ciangottini[a,b,2], L. Fanò[a,b], P. Lariccia[a,b], G. Mantovani[a,b], M. Menichelli[a], A. Saha[a], A. Santocchia[a,b], A. Spiezia[a,b,2]

INFN Sezione di Pisa [a]**, Università di Pisa** [b]**, Scuola Normale Superiore di Pisa** [c]**, Pisa, Italy**
K. Androsov[a,25], P. Azzurri[a], G. Bagliesi[a], J. Bernardini[a], T. Boccali[a], G. Broccolo[a,c], R. Castaldi[a], M.A. Ciocci[a,25], R. Dell'Orso[a], S. Donato[a,c,2], F. Fiori[a,c], L. Foà[a,c], A. Giassi[a], M.T. Grippo[a,25], F. Ligabue[a,c], T. Lomtadze[a], L. Martini[a,b], A. Messineo[a,b], C.S. Moon[a,26], F. Palla[a,2], A. Rizzi[a,b], A. Savoy-Navarro[a,27], A.T. Serban[a], P. Spagnolo[a], P. Squillacioti[a,25], R. Tenchini[a], G. Tonelli[a,b], A. Venturi[a], P.G. Verdini[a], C. Vernieri[a,c]

INFN Sezione di Roma [a]**, Università di Roma** [b]**, Roma, Italy**
L. Barone[a,b], F. Cavallari[a], G. D'imperio[a,b], D. Del Re[a,b], M. Diemoz[a], C. Jorda[a], E. Longo[a,b], F. Margaroli[a,b], P. Meridiani[a], F. Micheli[a,b,2], G. Organtini[a,b], R. Paramatti[a], S. Rahatlou[a,b], C. Rovelli[a], F. Santanastasio[a,b], L. Soffi[a,b], P. Traczyk[a,b,2]

INFN Sezione di Torino [a]**, Università di Torino** [b]**, Università del Piemonte Orientale (Novara)** [c]**, Torino, Italy**
N. Amapane[a,b], R. Arcidiacono[a,c], S. Argiro[a,b], M. Arneodo[a,c], R. Bellan[a,b], C. Biino[a], N. Cartiglia[a], S. Casasso[a,b,2], M. Costa[a,b], A. Degano[a,b], N. Demaria[a], L. Finco[a,b,2], C. Mariotti[a], S. Maselli[a], E. Migliore[a,b], V. Monaco[a,b], M. Musich[a], M.M. Obertino[a,c], L. Pacher[a,b], N. Pastrone[a], M. Pelliccioni[a], G.L. Pinna Angioni[a,b], A. Potenza[a,b], A. Romero[a,b], M. Ruspa[a,c], R. Sacchi[a,b], A. Solano[a,b], A. Staiano[a], U. Tamponi[a]

INFN Sezione di Trieste [a]**, Università di Trieste** [b]**, Trieste, Italy**
S. Belforte[a], V. Candelise[a,b,2], M. Casarsa[a], F. Cossutti[a], G. Della Ricca[a,b], B. Gobbo[a], C. La Licata[a,b], M. Marone[a,b], A. Schizzi[a,b], T. Umer[a,b], A. Zanetti[a]

Kangwon National University, Chunchon, Korea
S. Chang, A. Kropivnitskaya, S.K. Nam

Kyungpook National University, Daegu, Korea
D.H. Kim, G.N. Kim, M.S. Kim, D.J. Kong, S. Lee, Y.D. Oh, H. Park, A. Sakharov, D.C. Son

Chonbuk National University, Jeonju, Korea
T.J. Kim, M.S. Ryu

Chonnam National University, Institute for Universe and Elementary Particles, Kwangju, Korea
J.Y. Kim, D.H. Moon, S. Song

Korea University, Seoul, Korea
S. Choi, D. Gyun, B. Hong, M. Jo, H. Kim, Y. Kim, B. Lee, K.S. Lee, S.K. Park, Y. Roh

Seoul National University, Seoul, Korea
H.D. Yoo

University of Seoul, Seoul, Korea
M. Choi, J.H. Kim, I.C. Park, G. Ryu

Sungkyunkwan University, Suwon, Korea
Y. Choi, Y.K. Choi, J. Goh, D. Kim, E. Kwon, J. Lee, I. Yu

Vilnius University, Vilnius, Lithuania
A. Juodagalvis

National Centre for Particle Physics, Universiti Malaya, Kuala Lumpur, Malaysia
J.R. Komaragiri, M.A.B. Md Ali

Centro de Investigacion y de Estudios Avanzados del IPN, Mexico City, Mexico
E. Casimiro Linares, H. Castilla-Valdez, E. De La Cruz-Burelo, I. Heredia-de La Cruz,
A. Hernandez-Almada, R. Lopez-Fernandez, A. Sanchez-Hernandez

Universidad Iberoamericana, Mexico City, Mexico
S. Carrillo Moreno, F. Vazquez Valencia

Benemerita Universidad Autonoma de Puebla, Puebla, Mexico
I. Pedraza, H.A. Salazar Ibarguen

Universidad Autónoma de San Luis Potosí, San Luis Potosí, Mexico
A. Morelos Pineda

University of Auckland, Auckland, New Zealand
D. Krofcheck

University of Canterbury, Christchurch, New Zealand
P.H. Butler, S. Reucroft

National Centre for Physics, Quaid-I-Azam University, Islamabad, Pakistan
A. Ahmad, M. Ahmad, Q. Hassan, H.R. Hoorani, W.A. Khan, T. Khurshid, M. Shoaib

National Centre for Nuclear Research, Swierk, Poland
H. Bialkowska, M. Bluj, B. Boimska, T. Frueboes, M. Górski, M. Kazana, K. Nawrocki,
K. Romanowska-Rybinska, M. Szleper, P. Zalewski

Institute of Experimental Physics, Faculty of Physics, University of Warsaw, Warsaw, Poland
G. Brona, K. Bunkowski, M. Cwiok, W. Dominik, K. Doroba, A. Kalinowski, M. Konecki,
J. Krolikowski, M. Misiura, M. Olszewski

Laboratório de Instrumentação e Física Experimental de Partículas, Lisboa, Portugal
P. Bargassa, C. Beirão Da Cruz E Silva, P. Faccioli, P.G. Ferreira Parracho, M. Gallinaro, L. Lloret
Iglesias, F. Nguyen, J. Rodrigues Antunes, J. Seixas, J. Varela, P. Vischia

Joint Institute for Nuclear Research, Dubna, Russia
S. Afanasiev, P. Bunin, M. Gavrilenko, I. Golutvin, I. Gorbunov, A. Kamenev, V. Karjavin,
V. Konoplyanikov, A. Lanev, A. Malakhov, V. Matveev[28], P. Moisenz, V. Palichik, V. Perelygin,
S. Shmatov, N. Skatchkov, V. Smirnov, A. Zarubin

Petersburg Nuclear Physics Institute, Gatchina (St. Petersburg), Russia
V. Golovtsov, Y. Ivanov, V. Kim[29], E. Kuznetsova, P. Levchenko, V. Murzin, V. Oreshkin,
I. Smirnov, V. Sulimov, L. Uvarov, S. Vavilov, A. Vorobyev, An. Vorobyev

Institute for Nuclear Research, Moscow, Russia
Yu. Andreev, A. Dermenev, S. Gninenko, N. Golubev, M. Kirsanov, N. Krasnikov, A. Pashenkov, D. Tlisov, A. Toropin

Institute for Theoretical and Experimental Physics, Moscow, Russia
V. Epshteyn, V. Gavrilov, N. Lychkovskaya, V. Popov, I. Pozdnyakov, G. Safronov, S. Semenov, A. Spiridonov, V. Stolin, E. Vlasov, A. Zhokin

P.N. Lebedev Physical Institute, Moscow, Russia
V. Andreev, M. Azarkin[30], I. Dremin[30], M. Kirakosyan, A. Leonidov[30], G. Mesyats, S.V. Rusakov, A. Vinogradov

Skobeltsyn Institute of Nuclear Physics, Lomonosov Moscow State University, Moscow, Russia
A. Belyaev, E. Boos, M. Dubinin[31], L. Dudko, A. Ershov, A. Gribushin, V. Klyukhin, O. Kodolova, I. Lokhtin, S. Obraztsov, S. Petrushanko, V. Savrin, A. Snigirev

State Research Center of Russian Federation, Institute for High Energy Physics, Protvino, Russia
I. Azhgirey, I. Bayshev, S. Bitioukov, V. Kachanov, A. Kalinin, D. Konstantinov, V. Krychkine, V. Petrov, R. Ryutin, A. Sobol, L. Tourtchanovitch, S. Troshin, N. Tyurin, A. Uzunian, A. Volkov

University of Belgrade, Faculty of Physics and Vinca Institute of Nuclear Sciences, Belgrade, Serbia
P. Adzic[32], M. Ekmedzic, J. Milosevic, V. Rekovic

Centro de Investigaciones Energéticas Medioambientales y Tecnológicas (CIEMAT), Madrid, Spain
J. Alcaraz Maestre, C. Battilana, E. Calvo, M. Cerrada, M. Chamizo Llatas, N. Colino, B. De La Cruz, A. Delgado Peris, D. Domínguez Vázquez, A. Escalante Del Valle, C. Fernandez Bedoya, J.P. Fernández Ramos, J. Flix, M.C. Fouz, P. Garcia-Abia, O. Gonzalez Lopez, S. Goy Lopez, J.M. Hernandez, M.I. Josa, E. Navarro De Martino, A. Pérez-Calero Yzquierdo, J. Puerta Pelayo, A. Quintario Olmeda, I. Redondo, L. Romero, M.S. Soares

Universidad Autónoma de Madrid, Madrid, Spain
C. Albajar, J.F. de Trocóniz, M. Missiroli, D. Moran

Universidad de Oviedo, Oviedo, Spain
H. Brun, J. Cuevas, J. Fernandez Menendez, S. Folgueras, I. Gonzalez Caballero

Instituto de Física de Cantabria (IFCA), CSIC-Universidad de Cantabria, Santander, Spain
J.A. Brochero Cifuentes, I.J. Cabrillo, A. Calderon, J. Duarte Campderros, M. Fernandez, G. Gomez, A. Graziano, A. Lopez Virto, J. Marco, R. Marco, C. Martinez Rivero, F. Matorras, F.J. Munoz Sanchez, J. Piedra Gomez, T. Rodrigo, A.Y. Rodríguez-Marrero, A. Ruiz-Jimeno, L. Scodellaro, I. Vila, R. Vilar Cortabitarte

CERN, European Organization for Nuclear Research, Geneva, Switzerland
D. Abbaneo, E. Auffray, G. Auzinger, M. Bachtis, P. Baillon, A.H. Ball, D. Barney, A. Benaglia, J. Bendavid, L. Benhabib, J.F. Benitez, P. Bloch, A. Bocci, A. Bonato, O. Bondu, C. Botta, H. Breuker, T. Camporesi, G. Cerminara, S. Colafranceschi[33], M. D'Alfonso, D. d'Enterria, A. Dabrowski, A. David, F. De Guio, A. De Roeck, S. De Visscher, E. Di Marco, M. Dobson, M. Dordevic, B. Dorney, N. Dupont-Sagorin, A. Elliott-Peisert, G. Franzoni, W. Funk, D. Gigi, K. Gill, D. Giordano, M. Girone, F. Glege, R. Guida, S. Gundacker, M. Guthoff, J. Hammer, M. Hansen, P. Harris, J. Hegeman, V. Innocente, P. Janot, K. Kousouris, K. Krajczar, P. Lecoq,

C. Lourenço, N. Magini, L. Malgeri, M. Mannelli, J. Marrouche, L. Masetti, F. Meijers, S. Mersi, E. Meschi, F. Moortgat, S. Morovic, M. Mulders, L. Orsini, L. Pape, E. Perez, A. Petrilli, G. Petrucciani, A. Pfeiffer, M. Pimiä, D. Piparo, M. Plagge, A. Racz, G. Rolandi[34], M. Rovere, H. Sakulin, C. Schäfer, C. Schwick, A. Sharma, P. Siegrist, P. Silva, M. Simon, P. Sphicas[35], D. Spiga, J. Steggemann, B. Stieger, M. Stoye, Y. Takahashi, D. Treille, A. Tsirou, G.I. Veres[17], N. Wardle, H.K. Wöhri, H. Wollny, W.D. Zeuner

Paul Scherrer Institut, Villigen, Switzerland
W. Bertl, K. Deiters, W. Erdmann, R. Horisberger, Q. Ingram, H.C. Kaestli, D. Kotlinski, U. Langenegger, D. Renker, T. Rohe

Institute for Particle Physics, ETH Zurich, Zurich, Switzerland
F. Bachmair, L. Bäni, L. Bianchini, M.A. Buchmann, B. Casal, N. Chanon, G. Dissertori, M. Dittmar, M. Donegà, M. Dünser, P. Eller, C. Grab, D. Hits, J. Hoss, W. Lustermann, B. Mangano, A.C. Marini, M. Marionneau, P. Martinez Ruiz del Arbol, M. Masciovecchio, D. Meister, N. Mohr, P. Musella, C. Nägeli[36], F. Nessi-Tedaldi, F. Pandolfi, F. Pauss, L. Perrozzi, M. Peruzzi, M. Quittnat, L. Rebane, M. Rossini, A. Starodumov[37], M. Takahashi, K. Theofilatos, R. Wallny, H.A. Weber

Universität Zürich, Zurich, Switzerland
C. Amsler[38], M.F. Canelli, V. Chiochia, A. De Cosa, A. Hinzmann, T. Hreus, B. Kilminster, C. Lange, B. Millan Mejias, J. Ngadiuba, D. Pinna, P. Robmann, F.J. Ronga, S. Taroni, M. Verzetti, Y. Yang

National Central University, Chung-Li, Taiwan
M. Cardaci, K.H. Chen, C. Ferro, C.M. Kuo, W. Lin, Y.J. Lu, R. Volpe, S.S. Yu

National Taiwan University (NTU), Taipei, Taiwan
P. Chang, Y.H. Chang, Y. Chao, K.F. Chen, P.H. Chen, C. Dietz, U. Grundler, W.-S. Hou, Y.F. Liu, R.-S. Lu, E. Petrakou, Y.M. Tzeng, R. Wilken

Chulalongkorn University, Faculty of Science, Department of Physics, Bangkok, Thailand
B. Asavapibhop, G. Singh, N. Srimanobhas, N. Suwonjandee

Cukurova University, Adana, Turkey
A. Adiguzel, M.N. Bakirci[39], S. Cerci[40], C. Dozen, I. Dumanoglu, E. Eskut, S. Girgis, G. Gokbulut, Y. Guler, E. Gurpinar, I. Hos, E.E. Kangal, A. Kayis Topaksu, G. Onengut[41], K. Ozdemir, S. Ozturk[39], A. Polatoz, D. Sunar Cerci[40], B. Tali[40], H. Topakli[39], M. Vergili, C. Zorbilmez

Middle East Technical University, Physics Department, Ankara, Turkey
I.V. Akin, B. Bilin, S. Bilmis, H. Gamsizkan[42], B. Isildak[43], G. Karapinar[44], K. Ocalan[45], S. Sekmen, U.E. Surat, M. Yalvac, M. Zeyrek

Bogazici University, Istanbul, Turkey
E.A. Albayrak[46], E. Gülmez, M. Kaya[47], O. Kaya[48], T. Yetkin[49]

Istanbul Technical University, Istanbul, Turkey
K. Cankocak, F.I. Vardarlı

National Scientific Center, Kharkov Institute of Physics and Technology, Kharkov, Ukraine
L. Levchuk, P. Sorokin

University of Bristol, Bristol, United Kingdom
J.J. Brooke, E. Clement, D. Cussans, H. Flacher, J. Goldstein, M. Grimes, G.P. Heath, H.F. Heath,

J. Jacob, L. Kreczko, C. Lucas, Z. Meng, D.M. Newbold[50], S. Paramesvaran, A. Poll, T. Sakuma, S. Seif El Nasr-storey, S. Senkin, V.J. Smith

Rutherford Appleton Laboratory, Didcot, United Kingdom
K.W. Bell, A. Belyaev[51], C. Brew, R.M. Brown, D.J.A. Cockerill, J.A. Coughlan, K. Harder, S. Harper, E. Olaiya, D. Petyt, C.H. Shepherd-Themistocleous, A. Thea, I.R. Tomalin, T. Williams, W.J. Womersley, S.D. Worm

Imperial College, London, United Kingdom
M. Baber, R. Bainbridge, O. Buchmuller, D. Burton, D. Colling, N. Cripps, P. Dauncey, G. Davies, M. Della Negra, P. Dunne, W. Ferguson, J. Fulcher, D. Futyan, G. Hall, G. Iles, M. Jarvis, G. Karapostoli, M. Kenzie, R. Lane, R. Lucas[50], L. Lyons, A.-M. Magnan, S. Malik, B. Mathias, J. Nash, A. Nikitenko[37], J. Pela, M. Pesaresi, K. Petridis, D.M. Raymond, S. Rogerson, A. Rose, C. Seez, P. Sharp[†], A. Tapper, M. Vazquez Acosta, T. Virdee, S.C. Zenz

Brunel University, Uxbridge, United Kingdom
J.E. Cole, P.R. Hobson, A. Khan, P. Kyberd, D. Leggat, D. Leslie, I.D. Reid, P. Symonds, L. Teodorescu, M. Turner

Baylor University, Waco, USA
J. Dittmann, K. Hatakeyama, A. Kasmi, H. Liu, T. Scarborough, Z. Wu

The University of Alabama, Tuscaloosa, USA
O. Charaf, S.I. Cooper, C. Henderson, P. Rumerio

Boston University, Boston, USA
A. Avetisyan, T. Bose, C. Fantasia, P. Lawson, C. Richardson, J. Rohlf, J. St. John, L. Sulak

Brown University, Providence, USA
J. Alimena, E. Berry, S. Bhattacharya, G. Christopher, D. Cutts, Z. Demiragli, N. Dhingra, A. Ferapontov, A. Garabedian, U. Heintz, G. Kukartsev, E. Laird, G. Landsberg, M. Luk, M. Narain, M. Segala, T. Sinthuprasith, T. Speer, J. Swanson

University of California, Davis, Davis, USA
R. Breedon, G. Breto, M. Calderon De La Barca Sanchez, S. Chauhan, M. Chertok, J. Conway, R. Conway, P.T. Cox, R. Erbacher, M. Gardner, W. Ko, R. Lander, M. Mulhearn, D. Pellett, J. Pilot, F. Ricci-Tam, S. Shalhout, J. Smith, M. Squires, D. Stolp, M. Tripathi, S. Wilbur, R. Yohay

University of California, Los Angeles, USA
R. Cousins, P. Everaerts, C. Farrell, J. Hauser, M. Ignatenko, G. Rakness, E. Takasugi, V. Valuev, M. Weber

University of California, Riverside, Riverside, USA
K. Burt, R. Clare, J. Ellison, J.W. Gary, G. Hanson, J. Heilman, M. Ivova Rikova, P. Jandir, E. Kennedy, F. Lacroix, O.R. Long, A. Luthra, M. Malberti, M. Olmedo Negrete, A. Shrinivas, S. Sumowidagdo, S. Wimpenny

University of California, San Diego, La Jolla, USA
J.G. Branson, G.B. Cerati, S. Cittolin, R.T. D'Agnolo, A. Holzner, R. Kelley, D. Klein, J. Letts, I. Macneill, D. Olivito, S. Padhi, C. Palmer, M. Pieri, M. Sani, V. Sharma, S. Simon, M. Tadel, Y. Tu, A. Vartak, C. Welke, F. Würthwein, A. Yagil

University of California, Santa Barbara, Santa Barbara, USA
D. Barge, J. Bradmiller-Feld, C. Campagnari, T. Danielson, A. Dishaw, V. Dutta, K. Flowers,

M. Franco Sevilla, P. Geffert, C. George, F. Golf, L. Gouskos, J. Incandela, C. Justus, N. Mccoll, J. Richman, D. Stuart, W. To, C. West, J. Yoo

California Institute of Technology, Pasadena, USA
A. Apresyan, A. Bornheim, J. Bunn, Y. Chen, J. Duarte, A. Mott, H.B. Newman, C. Pena, M. Pierini, M. Spiropulu, J.R. Vlimant, R. Wilkinson, S. Xie, R.Y. Zhu

Carnegie Mellon University, Pittsburgh, USA
V. Azzolini, A. Calamba, B. Carlson, T. Ferguson, Y. Iiyama, M. Paulini, J. Russ, H. Vogel, I. Vorobiev

University of Colorado at Boulder, Boulder, USA
J.P. Cumalat, W.T. Ford, A. Gaz, M. Krohn, E. Luiggi Lopez, U. Nauenberg, J.G. Smith, K. Stenson, S.R. Wagner

Cornell University, Ithaca, USA
J. Alexander, A. Chatterjee, J. Chaves, J. Chu, S. Dittmer, N. Eggert, N. Mirman, G. Nicolas Kaufman, J.R. Patterson, A. Ryd, E. Salvati, L. Skinnari, W. Sun, W.D. Teo, J. Thom, J. Thompson, J. Tucker, Y. Weng, L. Winstrom, P. Wittich

Fairfield University, Fairfield, USA
D. Winn

Fermi National Accelerator Laboratory, Batavia, USA
S. Abdullin, M. Albrow, J. Anderson, G. Apollinari, L.A.T. Bauerdick, A. Beretvas, J. Berryhill, P.C. Bhat, G. Bolla, K. Burkett, J.N. Butler, H.W.K. Cheung, F. Chlebana, S. Cihangir, V.D. Elvira, I. Fisk, J. Freeman, E. Gottschalk, L. Gray, D. Green, S. Grünendahl, O. Gutsche, J. Hanlon, D. Hare, R.M. Harris, J. Hirschauer, B. Hooberman, S. Jindariani, M. Johnson, U. Joshi, B. Klima, B. Kreis, S. Kwan[†], J. Linacre, D. Lincoln, R. Lipton, T. Liu, J. Lykken, K. Maeshima, J.M. Marraffino, V.I. Martinez Outschoorn, S. Maruyama, D. Mason, P. McBride, P. Merkel, K. Mishra, S. Mrenna, S. Nahn, C. Newman-Holmes, V. O'Dell, O. Prokofyev, E. Sexton-Kennedy, S. Sharma, A. Soha, W.J. Spalding, L. Spiegel, L. Taylor, S. Tkaczyk, N.V. Tran, L. Uplegger, E.W. Vaandering, R. Vidal, A. Whitbeck, J. Whitmore, F. Yang

University of Florida, Gainesville, USA
D. Acosta, P. Avery, P. Bortignon, D. Bourilkov, M. Carver, D. Curry, S. Das, M. De Gruttola, G.P. Di Giovanni, R.D. Field, M. Fisher, I.K. Furic, J. Hugon, J. Konigsberg, A. Korytov, T. Kypreos, J.F. Low, K. Matchev, H. Mei, P. Milenovic[52], G. Mitselmakher, L. Muniz, A. Rinkevicius, L. Shchutska, M. Snowball, D. Sperka, J. Yelton, M. Zakaria

Florida International University, Miami, USA
S. Hewamanage, S. Linn, P. Markowitz, G. Martinez, J.L. Rodriguez

Florida State University, Tallahassee, USA
T. Adams, A. Askew, J. Bochenek, B. Diamond, J. Haas, S. Hagopian, V. Hagopian, K.F. Johnson, H. Prosper, V. Veeraraghavan, M. Weinberg

Florida Institute of Technology, Melbourne, USA
M.M. Baarmand, M. Hohlmann, H. Kalakhety, F. Yumiceva

University of Illinois at Chicago (UIC), Chicago, USA
M.R. Adams, L. Apanasevich, D. Berry, R.R. Betts, I. Bucinskaite, R. Cavanaugh, O. Evdokimov, L. Gauthier, C.E. Gerber, D.J. Hofman, P. Kurt, C. O'Brien, I.D. Sandoval Gonzalez, C. Silkworth, P. Turner, N. Varelas

The University of Iowa, Iowa City, USA
B. Bilki[53], W. Clarida, K. Dilsiz, M. Haytmyradov, J.-P. Merlo, H. Mermerkaya[54], A. Mestvirishvili, A. Moeller, J. Nachtman, H. Ogul, Y. Onel, F. Ozok[46], A. Penzo, R. Rahmat, S. Sen, P. Tan, E. Tiras, J. Wetzel, K. Yi

Johns Hopkins University, Baltimore, USA
I. Anderson, B.A. Barnett, B. Blumenfeld, S. Bolognesi, D. Fehling, A.V. Gritsan, P. Maksimovic, C. Martin, M. Swartz

The University of Kansas, Lawrence, USA
P. Baringer, A. Bean, G. Benelli, C. Bruner, J. Gray, R.P. Kenny III, D. Majumder, M. Malek, M. Murray, D. Noonan, S. Sanders, J. Sekaric, R. Stringer, Q. Wang, J.S. Wood

Kansas State University, Manhattan, USA
I. Chakaberia, A. Ivanov, K. Kaadze, S. Khalil, M. Makouski, Y. Maravin, L.K. Saini, N. Skhirtladze, I. Svintradze

Lawrence Livermore National Laboratory, Livermore, USA
J. Gronberg, D. Lange, F. Rebassoo, D. Wright

University of Maryland, College Park, USA
A. Baden, A. Belloni, B. Calvert, S.C. Eno, J.A. Gomez, N.J. Hadley, R.G. Kellogg, T. Kolberg, Y. Lu, A.C. Mignerey, K. Pedro, A. Skuja, M.B. Tonjes, S.C. Tonwar

Massachusetts Institute of Technology, Cambridge, USA
A. Apyan, R. Barbieri, W. Busza, I.A. Cali, M. Chan, L. Di Matteo, G. Gomez Ceballos, M. Goncharov, D. Gulhan, M. Klute, Y.S. Lai, Y.-J. Lee, A. Levin, P.D. Luckey, C. Paus, D. Ralph, C. Roland, G. Roland, G.S.F. Stephans, K. Sumorok, D. Velicanu, J. Veverka, B. Wyslouch, M. Yang, M. Zanetti, V. Zhukova

University of Minnesota, Minneapolis, USA
B. Dahmes, A. Gude, S.C. Kao, K. Klapoetke, Y. Kubota, J. Mans, S. Nourbakhsh, N. Pastika, R. Rusack, A. Singovsky, N. Tambe, J. Turkewitz

University of Mississippi, Oxford, USA
J.G. Acosta, S. Oliveros

University of Nebraska-Lincoln, Lincoln, USA
E. Avdeeva, K. Bloom, S. Bose, D.R. Claes, A. Dominguez, R. Gonzalez Suarez, J. Keller, D. Knowlton, I. Kravchenko, J. Lazo-Flores, F. Meier, F. Ratnikov, G.R. Snow, M. Zvada

State University of New York at Buffalo, Buffalo, USA
J. Dolen, A. Godshalk, I. Iashvili, A. Kharchilava, A. Kumar, S. Rappoccio

Northeastern University, Boston, USA
G. Alverson, E. Barberis, D. Baumgartel, M. Chasco, A. Massironi, D.M. Morse, D. Nash, T. Orimoto, D. Trocino, R.-J. Wang, D. Wood, J. Zhang

Northwestern University, Evanston, USA
K.A. Hahn, A. Kubik, N. Mucia, N. Odell, B. Pollack, A. Pozdnyakov, M. Schmitt, S. Stoynev, K. Sung, M. Velasco, S. Won

University of Notre Dame, Notre Dame, USA
A. Brinkerhoff, K.M. Chan, A. Drozdetskiy, M. Hildreth, C. Jessop, D.J. Karmgard, N. Kellams, K. Lannon, S. Lynch, N. Marinelli, Y. Musienko[28], T. Pearson, M. Planer, R. Ruchti, G. Smith, N. Valls, M. Wayne, M. Wolf, A. Woodard

The Ohio State University, Columbus, USA

L. Antonelli, J. Brinson, B. Bylsma, L.S. Durkin, S. Flowers, A. Hart, C. Hill, R. Hughes, K. Kotov, T.Y. Ling, W. Luo, D. Puigh, M. Rodenburg, B.L. Winer, H. Wolfe, H.W. Wulsin

Princeton University, Princeton, USA

O. Driga, P. Elmer, J. Hardenbrook, P. Hebda, S.A. Koay, P. Lujan, D. Marlow, T. Medvedeva, M. Mooney, J. Olsen, P. Piroué, X. Quan, H. Saka, D. Stickland[2], C. Tully, J.S. Werner, A. Zuranski

University of Puerto Rico, Mayaguez, USA

E. Brownson, S. Malik, H. Mendez, J.E. Ramirez Vargas

Purdue University, West Lafayette, USA

V.E. Barnes, D. Benedetti, D. Bortoletto, M. De Mattia, L. Gutay, Z. Hu, M.K. Jha, M. Jones, K. Jung, M. Kress, N. Leonardo, D.H. Miller, N. Neumeister, B.C. Radburn-Smith, X. Shi, I. Shipsey, D. Silvers, A. Svyatkovskiy, F. Wang, W. Xie, L. Xu, J. Zablocki

Purdue University Calumet, Hammond, USA

N. Parashar, J. Stupak

Rice University, Houston, USA

A. Adair, B. Akgun, K.M. Ecklund, F.J.M. Geurts, W. Li, B. Michlin, B.P. Padley, R. Redjimi, J. Roberts, J. Zabel

University of Rochester, Rochester, USA

B. Betchart, A. Bodek, R. Covarelli, P. de Barbaro, R. Demina, Y. Eshaq, T. Ferbel, A. Garcia-Bellido, P. Goldenzweig, J. Han, A. Harel, O. Hindrichs, A. Khukhunaishvili, S. Korjenevski, G. Petrillo, D. Vishnevskiy

The Rockefeller University, New York, USA

R. Ciesielski, L. Demortier, K. Goulianos, C. Mesropian

Rutgers, The State University of New Jersey, Piscataway, USA

S. Arora, A. Barker, J.P. Chou, C. Contreras-Campana, E. Contreras-Campana, D. Duggan, D. Ferencek, Y. Gershtein, R. Gray, E. Halkiadakis, D. Hidas, S. Kaplan, A. Lath, S. Panwalkar, M. Park, R. Patel, S. Salur, S. Schnetzer, D. Sheffield, S. Somalwar, R. Stone, S. Thomas, P. Thomassen, M. Walker

University of Tennessee, Knoxville, USA

K. Rose, S. Spanier, A. York

Texas A&M University, College Station, USA

O. Bouhali[55], A. Castaneda Hernandez, R. Eusebi, W. Flanagan, J. Gilmore, T. Kamon[56], V. Khotilovich, V. Krutelyov, R. Montalvo, I. Osipenkov, Y. Pakhotin, A. Perloff, J. Roe, A. Rose, A. Safonov, I. Suarez, A. Tatarinov, K.A. Ulmer

Texas Tech University, Lubbock, USA

N. Akchurin, C. Cowden, J. Damgov, C. Dragoiu, P.R. Dudero, J. Faulkner, K. Kovitanggoon, S. Kunori, S.W. Lee, T. Libeiro, I. Volobouev

Vanderbilt University, Nashville, USA

E. Appelt, A.G. Delannoy, S. Greene, A. Gurrola, W. Johns, C. Maguire, Y. Mao, A. Melo, M. Sharma, P. Sheldon, B. Snook, S. Tuo, J. Velkovska

University of Virginia, Charlottesville, USA
M.W. Arenton, S. Boutle, B. Cox, B. Francis, J. Goodell, R. Hirosky, A. Ledovskoy, H. Li, C. Lin, C. Neu, J. Wood

Wayne State University, Detroit, USA
C. Clarke, R. Harr, P.E. Karchin, C. Kottachchi Kankanamge Don, P. Lamichhane, J. Sturdy

University of Wisconsin, Madison, USA
D.A. Belknap, D. Carlsmith, M. Cepeda, S. Dasu, L. Dodd, S. Duric, E. Friis, R. Hall-Wilton, M. Herndon, A. Hervé, P. Klabbers, A. Lanaro, C. Lazaridis, A. Levine, R. Loveless, A. Mohapatra, I. Ojalvo, T. Perry, G.A. Pierro, G. Polese, I. Ross, T. Sarangi, A. Savin, W.H. Smith, D. Taylor, C. Vuosalo, N. Woods

†: Deceased
1: Also at Vienna University of Technology, Vienna, Austria
2: Also at CERN, European Organization for Nuclear Research, Geneva, Switzerland
3: Also at Institut Pluridisciplinaire Hubert Curien, Université de Strasbourg, Université de Haute Alsace Mulhouse, CNRS/IN2P3, Strasbourg, France
4: Also at National Institute of Chemical Physics and Biophysics, Tallinn, Estonia
5: Also at Skobeltsyn Institute of Nuclear Physics, Lomonosov Moscow State University, Moscow, Russia
6: Also at Universidade Estadual de Campinas, Campinas, Brazil
7: Also at Laboratoire Leprince-Ringuet, Ecole Polytechnique, IN2P3-CNRS, Palaiseau, France
8: Also at Joint Institute for Nuclear Research, Dubna, Russia
9: Also at Suez University, Suez, Egypt
10: Also at British University in Egypt, Cairo, Egypt
11: Also at Cairo University, Cairo, Egypt
12: Also at Ain Shams University, Cairo, Egypt
13: Now at Sultan Qaboos University, Muscat, Oman
14: Also at Université de Haute Alsace, Mulhouse, France
15: Also at Brandenburg University of Technology, Cottbus, Germany
16: Also at Institute of Nuclear Research ATOMKI, Debrecen, Hungary
17: Also at Eötvös Loránd University, Budapest, Hungary
18: Also at University of Debrecen, Debrecen, Hungary
19: Also at University of Visva-Bharati, Santiniketan, India
20: Now at King Abdulaziz University, Jeddah, Saudi Arabia
21: Also at University of Ruhuna, Matara, Sri Lanka
22: Also at Isfahan University of Technology, Isfahan, Iran
23: Also at University of Tehran, Department of Engineering Science, Tehran, Iran
24: Also at Plasma Physics Research Center, Science and Research Branch, Islamic Azad University, Tehran, Iran
25: Also at Università degli Studi di Siena, Siena, Italy
26: Also at Centre National de la Recherche Scientifique (CNRS) - IN2P3, Paris, France
27: Also at Purdue University, West Lafayette, USA
28: Also at Institute for Nuclear Research, Moscow, Russia
29: Also at St. Petersburg State Polytechnical University, St. Petersburg, Russia
30: Also at National Research Nuclear University "Moscow Engineering Physics Institute" (MEPhI), Moscow, Russia
31: Also at California Institute of Technology, Pasadena, USA
32: Also at Faculty of Physics, University of Belgrade, Belgrade, Serbia
33: Also at Facoltà Ingegneria, Università di Roma, Roma, Italy

34: Also at Scuola Normale e Sezione dell'INFN, Pisa, Italy

35: Also at University of Athens, Athens, Greece

36: Also at Paul Scherrer Institut, Villigen, Switzerland

37: Also at Institute for Theoretical and Experimental Physics, Moscow, Russia

38: Also at Albert Einstein Center for Fundamental Physics, Bern, Switzerland

39: Also at Gaziosmanpasa University, Tokat, Turkey

40: Also at Adiyaman University, Adiyaman, Turkey

41: Also at Cag University, Mersin, Turkey

42: Also at Anadolu University, Eskisehir, Turkey

43: Also at Ozyegin University, Istanbul, Turkey

44: Also at Izmir Institute of Technology, Izmir, Turkey

45: Also at Necmettin Erbakan University, Konya, Turkey

46: Also at Mimar Sinan University, Istanbul, Istanbul, Turkey

47: Also at Marmara University, Istanbul, Turkey

48: Also at Kafkas University, Kars, Turkey

49: Also at Yildiz Technical University, Istanbul, Turkey

50: Also at Rutherford Appleton Laboratory, Didcot, United Kingdom

51: Also at School of Physics and Astronomy, University of Southampton, Southampton, United Kingdom

52: Also at University of Belgrade, Faculty of Physics and Vinca Institute of Nuclear Sciences, Belgrade, Serbia

53: Also at Argonne National Laboratory, Argonne, USA

54: Also at Erzincan University, Erzincan, Turkey

55: Also at Texas A&M University at Qatar, Doha, Qatar

56: Also at Kyungpook National University, Daegu, Korea